Fig. 7 Morphometric analyses of FUS-positive neuropil granules in the neocortex of the parahippocampal gyrus. Digital images were taken from FUS and haematoxylin-stained tissue sections of control subjects (**a**), FTLD-TDP patients Alzheimer's disease patients and an FTLD-FUS patient (**b**). Then, the nuclei were dissected out manually (**b** and **c**, *inset*) and the images were converted to a gray scale for quantitation. **c** FUS immunopositive pixels were counted and expressed as per cent of synaptophysin-positive pixels similarly counted in a nearby section. The results are shown as scatter plots. The *horizontal bars* indicate the mean values. *$p < 0.05$. The size of each image is 2,000 × 2,000 pixels. *Scale bar* 50 μm in **a**

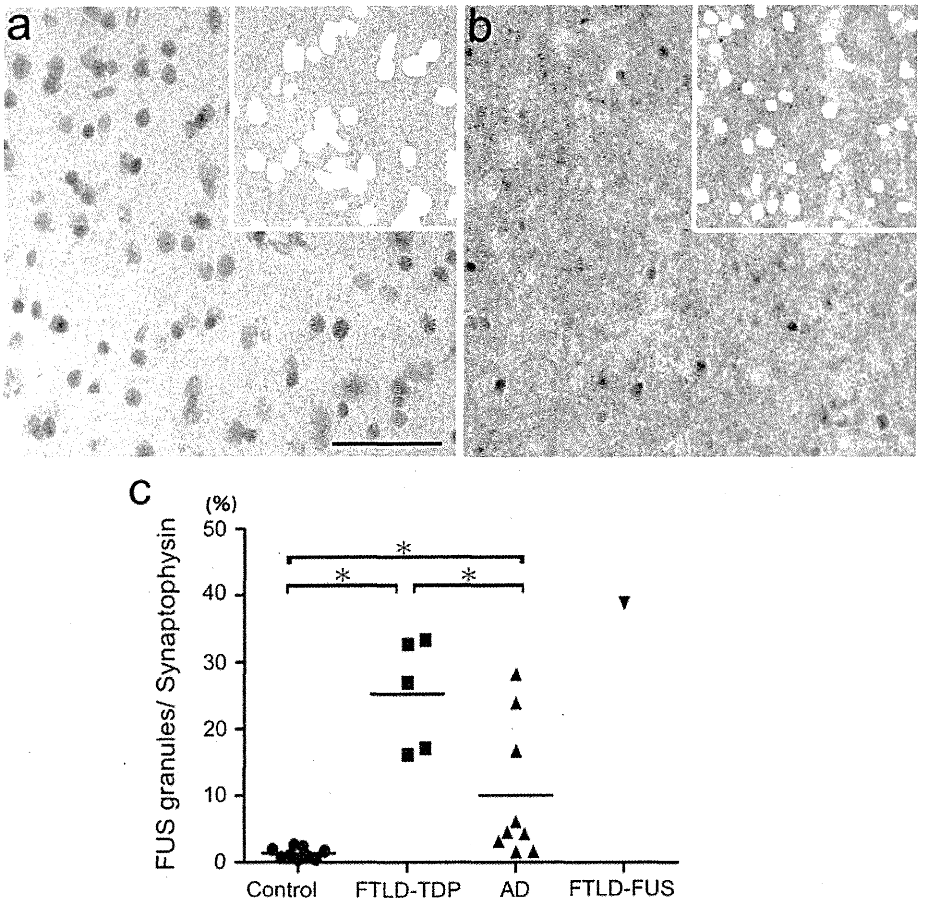

degenerative change, in addition to its physiological functions. In a cell biologic study, FUS was shown to be recruited, in response to stress stimuli that lead to apoptosis, to stress granules, a form of cytoplasmic RNA granules that are composed of RNA-binding proteins and mRNA [8]. The increased dendritic FUS, therefore, might be associated with stress responses in neurodegenerative diseases. On the other hand, in a study with Drosophila models, cytoplasmic but not nuclear localization of FUS was linked to cellular degeneration [22]. The more pronounced increase in FTLD-TDP than in AD suggests its association with some abnormality in the dendritic RNA translation in which both FUS and TDP-43 are involved. In this study, only one FTLD-FUS case was available and, therefore, the significance of the result from this case remains uncertain. Nevertheless, an extreme increase of FUS granules in this case might support a notion that such a change is associated with the pathogenesis or pathophysiology of these RNA-binding protein-associated neurodegenerative diseases. Whether or not our observations are related to a recent finding that accumulation of FUS granules in the cytoplasm of spinal anterior horn cells in familial ALS with FUS mutations [25] is an issue of significant interest.

In conclusion, the immunohistochemical study of lightly fixed, free-floating sections of postmortem brains has revealed that FUS resides, not only in the nucleus, but also in the dendrites. At least, a portion of such FUS-immunoreactivity is located in the post-synapses. The specific neuroanatomical distribution, which is similar in mouse and human, indicates a physiological role, in particular, in the brainstem where the expression is mostly constitutive. The increase in the cerebral cortex in diseased brains infers that dendritic FUS is also related to some pathological processes.

Acknowledgments The authors thank the patients and their families who made this research possible. We also thank Dr. Kenichi Oshima and Dr. Kazuhiro Niizato (Tokyo Metropolitan Matuzawa Hospital), Dr. Eizo Iseki (Juntendo Tokyo Koto Geriatric Medical Center) and Dr. Mitsumoto Onaya (National Hospital Organization Shimofusa Psychiatric Medical Center) to provide brain samples. This research was supported by Grants-in-Aid for Young Scientists, 23791008 (S.H.) of the Japan Society for the Promotion of Science; Grants-in-Aid from the Ministry of Health, Labor and Welfare10102894 and 10103470 (H.A.), and the Ministry of Education, Culture, Science 09019658 (H.A.), Japan.

References

1. (1997) Consensus recommendations for the postmortem diagnosis of Alzheimer's disease. The National Institute on Aging, and Reagan Institute Working Group on Diagnostic Criteria for the

Neuropathological Assessment of Alzheimer's Disease. Neurobiol Aging 18:S1–S2

2. Andersson MK, Stahlberg A, Arvidsson Y, Olofsson A, Semb H, Stenman G, Nilsson O, Aman P (2008) The multifunctional FUS, EWS and TAF15 proto-oncoproteins show cell type-specific expression patterns and involvement in cell spreading and stress response. BMC Cell Biol 9:37
3. Arai T, Hasegawa M, Akiyama H, Ikeda K, Nonaka T, Mori H, Mann D, Tsuchiya K, Yoshida M, Hashizume Y, Oda T (2006) TDP-43 is a component of ubiquitin-positive tau-negative inclusions in frontotemporal lobar degeneration and amyotrophic lateral sclerosis. Biochem Biophys Res Commun 351:602–611
4. Arai T, Mackenzie IR, Hasegawa M, Nonoka T, Niizato K, Tsuchiya K, Iritani S, Onaya M, Akiyama H (2009) Phosphorylated TDP-43 in Alzheimer's disease and dementia with Lewy bodies. Acta Neuropathol 117:125–136
5. Armstrong RA, Gearing M, Bigio EH, Cruz-Sanchez FF, Duyckaerts C, Mackenzie IR, Perry RH, Skullerud K, Yokoo H, Cairns NJ (2011) The spectrum and severity of FUS-immunoreactive inclusions in the frontal and temporal lobes of ten cases of neuronal intermediate filament inclusion disease. Acta Neuropathol 121:219–228
6. Belly A, Moreau-Gachelin F, Sadoul R, Goldberg Y (2005) Delocalization of the multifunctional RNA splicing factor TLS/FUS in hippocampal neurones: exclusion from the nucleus and accumulation in dendritic granules and spine heads. Neurosci Lett 379:152–157
7. Bian H, Grossman M (2007) Frontotemporal lobar degeneration: recent progress in antemortem diagnosis. Acta Neuropathol 114:23–29
8. Bosco DA, Lemay N, Ko HK, Zhou H, Burke C, Kwiatkowski TJ Jr, Sapp P, McKenna-Yasek D, Brown RH Jr, Hayward LJ (2010) Mutant FUS proteins that cause amyotrophic lateral sclerosis incorporate into stress granules. Hum Mol Genet 19:4160–4175
9. Bouvier D, Corera AT, Tremblay ME, Riad M, Chagnon M, Murai KK, Pasquale EB, Fon EA, Doucet G (2008) Pre-synaptic and post-synaptic localization of EphA4 and EphB2 in adult mouse forebrain. J Neurochem 106:682–695
10. Cairns NJ, Bigio EH, Mackenzie IR, Neumann M, Lee VM, Hatanpaa KJ, White CL 3rd, Schneider JA, Grinberg LT, Halliday G, Duyckaerts C, Lowe JS, Holm IE, Tolnay M, Okamoto K, Yokoo H, Murayama S, Woulfe J, Munoz DG, Dickson DW, Ince PG, Trojanowski JQ, Mann DM (2007) Neuropathologic diagnostic and nosologic criteria for frontotemporal lobar degeneration: consensus of the Consortium for Frontotemporal Lobar Degeneration. Acta Neuropathol 114:5–22
11. Dormann D, Rodde R, Edbauer D, Bentmann E, Fischer I, Hruscha A, Than ME, Mackenzie IR, Capell A, Schmid B, Neumann M, Haass C (2010) ALS-associated fused in sarcoma (FUS) mutations disrupt transportin-mediated nuclear import. EMBO J 29:2841–2857
12. Fujii R, Okabe S, Urushido T, Inoue K, Yoshimura A, Tachibana T, Nishikawa T, Hicks GG, Takumi T (2005) The RNA binding protein TLS is translocated to dendritic spines by mGluR5 activation and regulates spine morphology. Curr Biol 15:587–593
13. Fujii R, Takumi T (2005) TLS facilitates transport of mRNA encoding an actin-stabilizing protein to dendritic spines. J Cell Sci 118:5755–5765
14. Geser F, Brandmeir NJ, Kwong LK, Martinez-Lage M, Elman L, McCluskey L, Xie SX, Lee VM, Trojanowski JQ (2008) Evidence of multisystem disorder in whole-brain map of pathological TDP-43 in amyotrophic lateral sclerosis. Arch Neurol 65:636–641
15. Gitcho MA, Baloh RH, Chakraverty S, Mayo K, Norton JB, Levitch D, Hatanpaa KJ, White CL 3rd, Bigio EH, Caselli R, Baker M, Al-Lozi MT, Morris JC, Pestronk A, Rademakers R, Goate AM, Cairns NJ (2008) TDP-43 A315T mutation in familial motor neuron disease. Ann Neurol 63:535–538
16. Hahn CG, Banerjee A, Macdonald ML, Cho DS, Kamins J, Nie Z, Borgmann-Winter KE, Grosser T, Pizarro A, Ciccimaro E, Arnold SE, Wang HY, Blair IA (2009) The post-synaptic density of human postmortem brain tissues: an experimental study paradigm for neuropsychiatric illnesses. PLoS ONE 4:e5251
17. Higashi S, Iseki E, Minegishi M, Togo T, Kabuta T, Wada K (2010) GIGYF2 is present in endosomal compartments in the mammalian brains and enhances IGF-1-induced ERK1/2 activation. J Neurochem 115:423–437
18. Higashi S, Moore DJ, Minegishi M, Kasanuki K, Fujishiro H, Kabuta T, Togo T, Katsuse O, Uchikado H, Furukawa Y, Hino H, Kosaka K, Sato K, Arai H, Wada K, Iseki E (2011) Localization of MAP1-LC3 in vulnerable neurons and Lewy bodies in brains of patients with dementia with Lewy bodies. J Neuropathol Exp Neurol 70:264–280
19. Iida J, Nishimura W, Yao I, Hata Y (2002) Synaptic localization of membrane-associated guanylate kinase-interacting protein mediated by the pleckstrin homology domain. Eur J Neurosci 15:1493–1498
20. Kabashi E, Valdmanis PN, Dion P, Spiegelman D, McConkey BJ, Vande Velde C, Bouchard JP, Lacomblez L, Pochigaeva K, Salachas F, Pradat PF, Camu W, Meininger V, Dupre N, Rouleau GA (2008) TARDBP mutations in individuals with sporadic and familial amyotrophic lateral sclerosis. Nat Genet 40:572–574
21. Kwiatkowski TJ Jr, Bosco DA, Leclerc AL, Tamrazian E, Vanderburg CR, Russ C, Davis A, Gilchrist J, Kasarskis EJ, Munsat T, Valdmanis P, Rouleau GA, Hosler BA, Cortelli P, de Jong PJ, Yoshinaga Y, Haines JL, Pericak-Vance MA, Yan J, Ticozzi N, Siddique T, McKenna-Yasek D, Sapp PC, Horvitz HR, Landers JE, Brown RH Jr (2009) Mutations in the FUS/TLS gene on chromosome 16 cause familial amyotrophic lateral sclerosis. Science 323:1205–1208
22. Lanson NA Jr, Maltare A, King H, Smith R, Kim JH, Taylor JP, Lloyd TE, Pandey UB (2011) A Drosophila model of FUS-related neurodegeneration reveals genetic interaction between FUS and TDP-43. Hum Mol Genet 20:2510–2523
23. Lashley T, Rohrer JD, Bandopadhyay R, Fry C, Ahmed Z, Isaacs AM, Brelstaff JH, Borroni B, Warren JD, Troakes C, King A, Al-Saraj S, Newcombe J, Quinn N, Ostergaard K, Schroder HD, Bojsen-Moller M, Braendgaard H, Fox NC, Rossor MN, Lees AJ, Holton JL, Revesz T (2011) A comparative clinical, pathological, biochemical and genetic study of fused in sarcoma proteinopathies. Brain 134:2548–2564
24. Liu-Yesucevitz L, Bassell GJ, Gitler AD, Hart AC, Klann E, Richter JD, Warren ST, Wolozin B (2011) Local RNA translation at the synapse and in disease. J Neurosci 31:16086–16093
25. Mackenzie IR, Ansorge O, Strong M, Bilbao J, Zinman L, Ang LC, Baker M, Stewart H, Eisen A, Rademakers R, Neumann M (2011) Pathological heterogeneity in amyotrophic lateral sclerosis with FUS mutations: two distinct patterns correlating with disease severity and mutation. Acta Neuropathol 122:87–98
26. Mackenzie IR, Munoz DG, Kusaka H, Yokota O, Ishihara K, Roeber S, Kretzschmar HA, Cairns NJ, Neumann M (2011) Distinct pathological subtypes of FTLD-FUS. Acta Neuropathol 121:207–218
27. Mackenzie IR, Neumann M, Baborie A, Sampathu DM, Du Plessis D, Jaros E, Perry RH, Trojanowski JQ, Mann DM, Lee VM (2011) A harmonized classification system for FTLD-TDP pathology. Acta Neuropathol 122:111–113
28. Mackenzie IR, Neumann M, Bigio EH, Cairns NJ, Alafuzoff I, Kril J, Kovacs GG, Ghetti B, Halliday G, Holm IE, Ince PG, Kamphorst W, Revesz T, Rozemuller AJ, Kumar-Singh S, Akiyama H, Baborie A, Spina S, Dickson DW, Trojanowski JQ, Mann DM (2009) Nomenclature for neuropathologic subtypes of

frontotemporal lobar degeneration: consensus recommendations. Acta Neuropathol 117:15–18
29. Mackenzie IR, Neumann M, Bigio EH, Cairns NJ, Alafuzoff I, Kril J, Kovacs GG, Ghetti B, Halliday G, Holm IE, Ince PG, Kamphorst W, Revesz T, Rozemuller AJ, Kumar-Singh S, Akiyama H, Baborie A, Spina S, Dickson DW, Trojanowski JQ, Mann DM (2010) Nomenclature and nosology for neuropathologic subtypes of frontotemporal lobar degeneration: an update. Acta Neuropathol 119:1–4
30. Munoz DG, Neumann M, Kusaka H, Yokota O, Ishihara K, Terada S, Kuroda S, Mackenzie IR (2009) FUS pathology in basophilic inclusion body disease. Acta Neuropathol 118:617–627
31. Neary D, Snowden JS, Gustafson L, Passant U, Stuss D, Black S, Freedman M, Kertesz A, Robert PH, Albert M, Boone K, Miller BL, Cummings J, Benson DF (1998) Frontotemporal lobar degeneration: a consensus on clinical diagnostic criteria. Neurology 51:1546–1554
32. Neumann M, Rademakers R, Roeber S, Baker M, Kretzschmar HA, Mackenzie IR (2009) A new subtype of frontotemporal lobar degeneration with FUS pathology. Brain 132:2922–2931
33. Neumann M, Roeber S, Kretzschmar HA, Rademakers R, Baker M, Mackenzie IR (2009) Abundant FUS-immunoreactive pathology in neuronal intermediate filament inclusion disease. Acta Neuropathol 118:605–616
34. Neumann M, Sampathu DM, Kwong LK, Truax AC, Micsenyi MC, Chou TT, Bruce J, Schuck T, Grossman M, Clark CM, McCluskey LF, Miller BL, Masliah E, Mackenzie IR, Feldman H, Feiden W, Kretzschmar HA, Trojanowski JQ, Lee VM (2006) Ubiquitinated TDP-43 in frontotemporal lobar degeneration and amyotrophic lateral sclerosis. Science 314:130–133
35. Prasad DD, Ouchida M, Lee L, Rao VN, Reddy ES (1994) TLS/FUS fusion domain of TLS/FUS-erg chimeric protein resulting from the t(16;21) chromosomal translocation in human myeloid leukemia functions as a transcriptional activation domain. Oncogene 9:3717–3729
36. Ringholz GM, Appel SH, Bradshaw M, Cooke NA, Mosnik DM, Schulz PE (2005) Prevalence and patterns of cognitive impairment in sporadic ALS. Neurology 65:586–590
37. Rosso SM, Donker Kaat L, Baks T, Joosse M, de Koning I, Pijnenburg Y, de Jong D, Dooijes D, Kamphorst W, Ravid R, Niermeijer MF, Verheij F, Kremer HP, Scheltens P, van Duijn CM, Heutink P, van Swieten JC (2003) Frontotemporal dementia in The Netherlands: patient characteristics and prevalence estimates from a population-based study. Brain 126:2016–2022
38. Sreedharan J, Blair IP, Tripathi VB, Hu X, Vance C, Rogelj B, Ackerley S, Durnall JC, Williams KL, Buratti E, Baralle F, de Belleroche J, Mitchell JD, Leigh PN, Al-Chalabi A, Miller CC, Nicholson G, Shaw CE (2008) TDP-43 mutations in familial and sporadic amyotrophic lateral sclerosis. Science 319:1668–1672
39. The Lund and Manchester Groups (1994) Clinical and neuropathological criteria for frontotemporal dementia. J Neurol Neurosurg Psychiatry 57:416–418
40. Van Deerlin VM, Leverenz JB, Bekris LM, Bird TD, Yuan W, Elman LB, Clay D, Wood EM, Chen-Plotkin AS, Martinez-Lage M, Steinbart E, McCluskey L, Grossman M, Neumann M, Wu IL, Yang WS, Kalb R, Galasko DR, Montine TJ, Trojanowski JQ, Lee VM, Schellenberg GD, Yu CE (2008) TARDBP mutations in amyotrophic lateral sclerosis with TDP-43 neuropathology: a genetic and histopathological analysis. Lancet Neurol 7:409–416
41. Vance C, Rogelj B, Hortobagyi T, De Vos KJ, Nishimura AL, Sreedharan J, Hu X, Smith B, Ruddy D, Wright P, Ganesalingam J, Williams KL, Tripathi V, Al-Saraj S, Al-Chalabi A, Leigh PN, Blair IP, Nicholson G, de Belleroche J, Gallo JM, Miller CC, Shaw CE (2009) Mutations in FUS, an RNA processing protein, cause familial amyotrophic lateral sclerosis type 6. Science 323:1208–1211
42. Wang HY, Wang IF, Bose J, Shen CK (2004) Structural diversity and functional implications of the eukaryotic TDP gene family. Genomics 83:130–139
43. Yokoseki A, Shiga A, Tan CF, Tagawa A, Kaneko H, Koyama A, Eguchi H, Tsujino A, Ikeuchi T, Kakita A, Okamoto K, Nishizawa M, Takahashi H, Onodera O (2008) TDP-43 mutation in familial amyotrophic lateral sclerosis. Ann Neurol 63:538–542
44. Zinszner H, Sok J, Immanuel D, Yin Y, Ron D (1997) TLS (FUS) binds RNA in vivo and engages in nucleo-cytoplasmic shuttling. J Cell Sci 110:1741–1750

Brain Advance Access published October 3, 2012
doi:10.1093/brain/aws230

BRAIN
A JOURNAL OF NEUROLOGY

Molecular analysis and biochemical classification of TDP-43 proteinopathy

Hiroshi Tsuji,[1,2] Tetsuaki Arai,[3,4] Fuyuki Kametani,[1] Takashi Nonaka,[1] Makiko Yamashita,[1] Masami Suzukake,[1] Masato Hosokawa,[3] Mari Yoshida,[5] Hiroyuki Hatsuta,[6] Masaki Takao,[6] Yuko Saito,[7] Shigeo Murayama,[6] Haruhiko Akiyama,[3] Masato Hasegawa,[1] David M. A. Mann[8] and Akira Tamaoka[2]

1 Department of Neuropathology and Cell Biology, Tokyo Metropolitan Institute of Medical Science, Tokyo 156-8585, Japan
2 Department of Neurology, Graduate School of Comprehensive Human Sciences, University of Tsukuba, Tsukuba-shi 305-8576, Japan
3 Department of Dementia and Higher Brain Function, Tokyo Metropolitan Institute of Medical Science, Tokyo 156-8585, Japan
4 Department of Psychiatry, Graduate School of Comprehensive Human Sciences, University of Tsukuba, Tsukuba-shi 305-8576, Japan
5 Department of Neuropathology, Institute for Medical Science of Aging, Aichi Medical University, Aichi 480-1195, Japan
6 Department of Neuropathology, Tokyo Metropolitan Institute of Gerontology, Tokyo 173-0015, Japan
7 Department of Pathology and Laboratory Medicine, National Center Hospital of Neurology and Psychiatry, Tokyo 187-8551, Japan
8 Mental Health and Neurodegeneration Research Group, Greater Manchester Neuroscience Centre, University of Manchester, Manchester M13 9PT, UK

Correspondence to: Masato Hasegawa,
Department of Neuropathology and Cell Biology,
Tokyo Metropolitan Institute of Medical Science,
2-1-6 Kamikitazawa,
Setagaya-ku,
Tokyo 156-8506,
Japan
E-mail: hasegawa-ms@igakuken.or.jp

Amyotrophic lateral sclerosis and frontotemporal lobar degeneration with TAR DNA-binding protein of 43 kDa pathology are progressive neurodegenerative diseases that are characterized by intracytoplasmic aggregates of hyperphosphorylated TAR DNA-binding protein of 43 kDa. These TAR DNA-binding protein 43 proteinopathies can be classified into subtypes, which are closely correlated with clinicopathological phenotypes, although the differences in the molecular species of TAR DNA-binding protein 43 in these diseases and the biological significance thereof, remain to be clarified. Here, we have shown that although the banding patterns of abnormally phosphorylated C-terminal fragments of TAR DNA-binding protein 43 differ between the neuropathological subtypes, these are indistinguishable between multiple brain regions and spinal cord in individual patients. Immunoblot analysis of protease-resistant TAR DNA-binding protein 43 demonstrated that the fragment patterns represent different conformations of TAR DNA-binding protein 43 molecular species in the diseases. These results suggest a new clinicopathological classification of TAR DNA-binding protein 43 proteinopathies based on their molecular properties.

Keywords: amyotrophic lateral sclerosis; frontotemporal lobar degeneration; TDP-43; classification

Abbreviations: ALS = amyotrophic lateral sclerosis; FTLD = frontotemporal lobar degeneration; FTLD-TDP = frontotemporal lobar degeneration with TAR DNA-binding protein of 43 kDa pathology; TDP-43 = TAR DNA-binding protein of 43 kDa

Received March 13, 2012. Revised June 3, 2012. Accepted June 28, 2012

Introduction

Amyotrophic lateral sclerosis (ALS) and frontotemporal lobar degeneration with TDP-43 pathology (FTLD-TDP) are sporadic and familial neurodegenerative diseases characterized neuropathologically by intracytoplasmic aggregates of TAR DNA-binding protein of 43 kDa (TDP-43) (Arai *et al.*, 2006; Neumann *et al.*, 2006). In ALS, upper and lower motor neurons progressively degenerate. Neuropathologically, the TDP-43-positive structures appear as rounded or skein-like inclusions in the lower motor neurons. Similar TDP-43-positive inclusions are also observed in the prefrontal gyrus that contains the upper motor neurons. Moreover, TDP-43-positive glial cytoplasmic inclusions are found close to the upper and lower motor neurons in ALS (Tan *et al.*, 2007). In FTLD-TDP, TDP-43 pathology is distinguished into four histological subtypes (types A–D) based on the predominant type of TDP-43-positive structures present (Mackenzie *et al.*, 2011). Type A is characterized by numerous short dystrophic neurites and crescentic or oval neuronal cytoplasmic inclusions; type B has moderate numbers of neuronal cytoplasmic inclusions, throughout all cortical layers, but few dystrophic neurites; type C has a predominance of elongated dystrophic neurites in upper cortical layers, with few neuronal cytoplasmic inclusions; and type D refers to the pathology associated with inclusion body myopathy with early onset Paget disease and frontotemporal dementia caused by *VCP* mutations, characterized by numerous short dystrophic neurites and frequent lentiform neuronal intranuclear inclusions. There is a relationship between subtypes of TDP-43 pathology and clinical phenotype, and many cases of ALS and frontotemporal lobar degeneration (FTLD) are readily distinguished by each clinical symptom. However, some cases have symptoms of both ALS and FTLD. ALS with dementia refers to cases initially presenting with motor neuron disease becoming demented, whereas FTLD-motor neuron disease refers to cases presenting with cognitive impairment and subsequently developing motor neuron disease.

TDP-43 pathology is also present in a subset of familial ALS and FTLD due to mutations in *TARDBP* (Kabashi *et al.*, 2008; Sreedharan *et al.*, 2008), progranulin (*GRN*; Baker *et al.*, 2006) and *C9ORF72* (DeJesus-Hernandez *et al.*, 2011; Renton *et al.*, 2011) genes. Although most patients with mutations in *TARDBP* present with ALS, some present with FTLD (Gitcho *et al.*, 2009; Kovacs *et al.*, 2009). Cases with FTLD-TDP with *GRN* mutation often show type A pathology (Mackenzie *et al.*, 2006b; Cairns *et al.*, 2007b; Josephs *et al.*, 2007). The pathology of ALS and FTLD due to mutations in *C9ORF72* is heterogeneous: TDP-43 pathology overlaps between ALS and FTLD-TDP types A and B (Murray *et al.*, 2011). One large multicentre study of sporadic and familial FTLD-TDP showed broad overlap between the TDP-43 subtyping, especially between types A and B (Armstrong *et al.*, 2010). These overlaps might occur because current pathological classification may be inadequate, as it is based solely on the morphological assessment of certain subjective cortical regions. A more objective and unbiased classification is needed.

In this study, we have investigated a wide range of patients with various TDP-43 proteinopathies to investigate whether patterns of protease-resistant TDP-43 might indicate different TDP-43 strain types, and characterize the TDP-43 C-terminal banding patterns in multiple regions of the CNS, basing our approach on the method used for demonstration of prion strain variation and the aetiology of new variant Creutzfeldt–Jakob disease (Collinge *et al.*, 1996). We show at least three C-terminal banding patterns that distinguish diseases with TDP-43 proteinopathy and report that the banding pattern in individual patients is indistinguishable in different brain regions and spinal cord. Corresponding patterns of protease-resistant phosphorylated TDP-43 are also seen between the pathological phenotypes. As with the prion diseases, the present results suggest that the different conformation of abnormal TDP-43 deposits in the CNS in patients corresponding with various subtypes of TDP-43 proteinopathy, and that the conformation state of the abnormal TDP-43 protein may determine the pathological phenotype.

Materials and methods

Patients

Human brain tissues were obtained from the Brain Donation Programme at the University of Tsukuba (Japan), Tokyo Metropolitan Institute of Gerontology (Japan), National Shimofusa Mental Hospital (Japan) and the University of Manchester (UK). This study was approved by the local Research Ethics Committee. The subjects in this study included eight patients with ALS, five patients with FTLD-TDP type A, eight patients with FTLD-TDP type B, six patients with FTLD-TDP type C and two patients with Alzheimer's disease without TDP-43 pathology. All cases with ALS met the revised El Escorial criteria for ALS (Brooks, 1994) without dementia. All cases with FTLD-TDP fulfilled clinical diagnostic criteria of FTLD (Neary *et al.*, 1998), and classifications of TDP-43 subtype were made in accordance with published guidelines (Cairns *et al.*, 2007*a*; Mackenzie *et al.*, 2011). Four patients with FTLD-TDP type A were cases of familial FTLD-U with *GRN* mutations. One familial ALS case, one with type A, and two with type B had the GGGCC repeat expansion in *C9ORF72*. The age, gender, brain regions examined and clinical diagnosis are given in Table 1.

A fresh frozen tissue sample was taken and cut into two pieces. One piece was fixed in 4% paraformaldehyde in 0.1 M phosphate buffer (pH 7.4) for 2 days and was used for immunohistochemical analysis. The other piece was homogenized and used for immunoblot analysis. In principle, we took the precentral gyrus and lumbar part of the spinal cord in the ALS cases, and the frontal lobe in the FTLD-TDP cases, because TDP-43 pathology is always known to be prevalent in these regions (Tan *et al.*, 2007; Geser *et al.*, 2008, 2009). However, the spinal cord was not available in four cases with ALS, and both motor regions in two cases were not available. In these cases, the frontal lobe was examined instead. For ALS Cases 1, 3, 5 and ALS and FTLD-TDP type C Case 22, the whole of the cerebral hemisphere and brainstem were available as fresh frozen tissues. In these four cases, we took the multiple regions, as described in Table 1. Every tissue sample was examined immunohistochemically for TDP-43-positive lesions. All samples, except some from the cerebellar cortex, showed an accumulation of abnormal TDP-43-positive structures.

Immunoblotting

Sarkosyl-insoluble, urea-soluble fractions were extracted from each region as previously described (Arai *et al.*, 2006; Hasegawa *et al.*, 2008).

Table 1 Description of the patients

Case number	Age at death (year)	Age at onset (year)	Sex	Family history	Brain weight (g)	Clinical diagnosis	Region
ALS							
1	62	61	M	N	1150	ALS	Prec, L and other regions[a]
2	72	71	F	N	1390	ALS	Prec and L
3	42	40	F	N	1140	ALS	Prec, L and other regions[a]
4	76	75	F	N	NA	ALS	Prec and L
5	62	54	M	N	1230	ALS	Prec and other regions[a]
6	77	76	F	N	NA	ALS	Prec
7	67	65	M	N	1414	ALS	Fr
8	55	53	M	Y(m*C9ORF72*)	1250	ALS	Fr
FTLD-TDP type A							
9	58	49	M	Y(m*C9ORF72*)	1050	FTD	Fr
10	67	54	F	Y(m*GRN*)	NA	FTD	Fr
11	71	63	F	Y(m*GRN*)	863	PNFA	Fr
12	66	56	F	Y(m*GRN*)	1100	FTD	Fr
13	68	60	M	Y(m*GRN*)	1210	FTD + MND	Fr
FTLD-TDP type B							
14	45	43	M	N	1260	FTD + MND	Fr
15	59	57	M	Y(m*C9ORF72*)	1210	FTD + MND	Fr
16	67	65	M	N	1280	FTD + MND	Fr
17	76	74	M	N	1215	FTD + MND	Fr
18	69	58	M	N	1166	FTD + MND	Fr
19	52	50	F	Y(m*C9ORF72*)	1050	FTD + MND	Fr
20	65	61	M	N	1530	FTD + MND	Fr
21	68	64	M	N	1213	FTD + MND	Fr
FTLD-TDP type C							
22	82	NA	M	N	1200	SD	Fr, Te and other regions[b]
23	67	65	M	N	NA	SD	Fr
24	59	53	M	N	NA	SD	Fr
25	63	58	M	N	NA	SD	Fr
26	66	55	F	N	1035	SD	Fr
27	75	60	M	N	1174	SD	Fr
AD							
28	65	56	F	N	1165	AD	Fr
29	70	NA	F	N	1126	AD	Fr

AD = Alzheimer's disease; Fr = frontal cortex; FTD = frontotemporal dementia; L = lumbar part of spinal cord; m*C9ORF72* = mutation of chromosome 9 open-reading frame 72 gene; m*GRN* = mutation of progranulin gene; MND = motor neuron disease; NA = not available; PNFA = progressive non-fluent aphasia; Prec = precentral gyrus; SD = semantic dementia; Y = yes; N = no.
a Other regions contained striatum, thalamus, hippocampus dentate gyrus, substantia nigra, pons, medulla and cerebellum cortex. In these cases, the grey and white matter of precentral gyrus were separated from each other macroscopically and examined.
b Other regions contain striatum, thalamus, hippocampus dentate gyrus, substantia nigra, pons, medulla and cerebellum cortex. FTLD-TDP type B without MND and type D are not analysed in this study.

The samples were loaded on 15% SDS–PAGE gels. Proteins in the gel were then transferred onto a polyvinylidene difluoride membrane (Millipore). After blocking with 3% gelatine in 0.01 M PBS (pH 7.4), membranes were incubated overnight with phosphorylation dependent anti-TDP-43 rabbit polyclonal antibody (pS409/410, 1:1000; Hasegawa *et al*., 2008), phosphorylation independent TDP-43 polyclonal antibody 10782-1-AP (TDP-43 pAb, 1:3000) and TDP-43 monoclonal antibody, 60019-2-Ig (TDP-43 mAb, 1:3000) (ProteinTech Group). After incubation with the appropriate biotinylated secondary antibody, immunolabelling was detected using the VECTASTAIN® ABC system (Vector Laboratories) coupled with a 3,3′-diaminobenzidine reaction intensified with nickel chloride. The blot membranes were digitally analysed, and densitometric analyses were performed with ImageJ version 1.44p (NIH, http://rsbweb.nih.gov/ij/index.html). The densitometry data were averaged for all cases in each group to illustrate the different patterns.

Immunohistochemistry

After cryoprotection in 15% sucrose in 0.01 M PBS (pH 7.4), paraformaldehyde-fixed tissue blocks were cut on a freezing microtome at 30-µm thickness. The free-floating sections were immunostained with phosphorylation-dependent TDP-43 monoclonal antibody (pS409/410, 1:10 000) (Inukai *et al*., 2008) for 72 h in the cold. After treatment with mouse secondary antibody, immunolabelling was detected using the VECTASTAIN ®ABC system coupled with a 3,3′-diaminobenzidine reaction to yield a brown precipitate. Sections were lightly counterstained with heamatoxylin.

Protease treatment of phosphorylated TDP-43

Sarkosyl-insoluble fractions extracted from the neocortical regions of patients with ALS or FTLD-TDP were treated with final concentration of 100 μg/ml trypsin (Promega) or 10 μg/ml chymotrypsin (Sigma-Aldrich) at 37°C for 30 min. The reaction was stopped by boiling for 5 min. After centrifuging at 15 000 rpm for 1 min, the samples were analysed by immunoblotting as described earlier.

Mass spectrometry

Sarkosyl-insoluble, trypsin-resistant fractions were loaded on 15% SDS–PAGE gels. The pS409/410-positive ~16 kDa bands were dissected and digested in-gel with chymotrypsin. The digests were applied to the Paradigm MS4 high-performance liquid chromatography system (Microm BioResources). A reversed phase capillary column (Develosil ODS-HG5, 0.075 × 150 mm, Nomura Chemical) was used at a flow rate of 300 nl/min with a 4–80% linear gradient of acetonitrile in 0.1% formic acid. Eluted peptides were directly detected with an ion trap mass spectrometer, LXQ (Thermo Fisher Scientific). The obtained spectra were analysed with Mascot (Matrix Science).

Statistical analysis

The *P*-values for the description of the statistical significance of differences were calculated by means of the paired, two-tailed *t*-test using Prism 5.04 software (GraphPad Software, Inc).

Results

Banding patterns of phosphorylated C-terminal TDP-43 in ALS and FTLD with TDP-43 pathology

Immunoblot analysis using an antibody specific for abnormal TDP-43, pS409/410, showed high-molecular-weight smearing substances, phosphorylated full-length TDP-43 at 45 kDa and several C-terminal fragments at 18–26 kDa to be present in affected brain regions in all cases (Fig. 1). Three major bands at 23, 24 and 26 kDa, and two minor bands at 18 and 19 kDa were seen in the precentral gyrus and frontal cortex of cases with ALS, with the 24 kDa band being the most intense (Fig. 1A and F). In the lumbar spinal cord, the two minor bands at 18 and 19 kDa were barely present, but the banding pattern of the three major bands at 23, 24 and 26 kDa was similar to that in the cerebral cortex (Fig. 1A). No such pS409/410-positive TDP-43 bands were detected in control cases with Alzheimer's disease with no TDP-43 pathology (Fig. 1B). In the FTLD-TDP cases, the banding pattern could be distinguished into three types according to the FTLD-TDP histological subtype (Fig. 1C–E). In FTLD-TDP type A, three major bands at 23, 24 and 26 kDa, and two minor bands at 18 and 19 kDa were detected, with the 23 kDa band being the most intense (Fig. 1C and F). In FTLD-type B cases, the banding pattern was the same as that in the ALS cases (Fig. 1D and F). In FTLD-TDP type C cases, two major bands at 23 and 24 kDa, and two minor bands at 18 and 19 kDa were detected, with the 24 kDa band being the most intense, and the band at 26 kDa being hardly detectable (Fig. 1E and F). Densitometric analyses of the immunoblots for all cases are shown in Supplementary Fig. 1. Each component of the C-terminal fragments was significantly different (Fig. 1F).

Immunoblot analysis using phosphorylation independent TDP-43 polyclonal and monoclonal antibodies detected phosphorylated full-length TDP-43 at 45 kDa, two bands ~25 kDa and high-molecular-weight smears, in addition to the normal TDP-43 band at 43 kDa in ALS and various subtypes of FTLD-TDP. The banding patterns between ALS and various subtypes of FTLD-TDP could not be distinguished with these antibodies. In the cases with Alzheimer's disease, the normal TDP-43 band at 43 kDa was detected, but neither the phosphorylated 45 kDa band nor the ~25 kDa fragments were observed (Supplementary Fig. 2). Immunoblot analysis of α-tubulin in Tris saline-soluble fractions from cases with types A, B and C pathology showed no correlation between the banding pattern of α-tubulin and that of TDP-43 (Supplementary Fig. 3), indicating that the differences in the banding patterns are not because of protein degradation caused by a long post-mortem interval or unfavourable agonal status.

Immunohistochemistry and immunoblot analyses of phosphorylated TDP-43 in multiple regions of ALS and FTLD with TDP-43 pathology

In ALS cases, the neuronal cytoplasmic pathology, which included skein-like inclusions, irregularly shaped TDP-immunoreactive neuronal cytoplasmic inclusions and densely staining granules, was confirmed in multiple regions by immunohistochemistry analysis using pS409/410 (Fig. 2A–G). Glial cytoplasmic inclusions were also present in many regions. Glial cytoplasmic inclusions were more frequent in the white matter than in the grey matter (Fig. 2H). A few neuronal cytoplasmic inclusions were found in the cerebellar cortex granule cells (Fig. 2G). In FTLD-TDP type C, dystrophic neurites were seen in multiple regions except for the cerebellar cortex (Fig. 2I–O), whereas neuronal cytoplasmic inclusions were also present in the striatum and hippocampus dentate gyrus granule cells (Fig. 2J and L). No abnormal structures were found in the cerebellar cortex (data not shown). These observations show that pathological TDP-43 is present throughout many CNS areas in ALS, suggesting that ALS does not selectively affect only the motor system, but it is rather a multisystem neurodegenerative TDP-43 proteinopathy.

Immunoblot analyses of three ALS cases confirmed that phosphorylated TDP-43 and the C-terminal fragments are deposited in multiple brain regions in ALS (Fig. 3A). Relatively strong immunoreactivities were detected in the striatum (in Cases 3 and 5) and substantia nigra (in Cases 1 and 5), although this varied between cases (Fig. 3A). Importantly, the banding pattern for the TDP-43 C-terminal fragments in these three cases was basically the same in all brain regions examined (Fig. 3A). In FTLD-TDP type C, a C-terminal banding pattern, clearly distinct from that

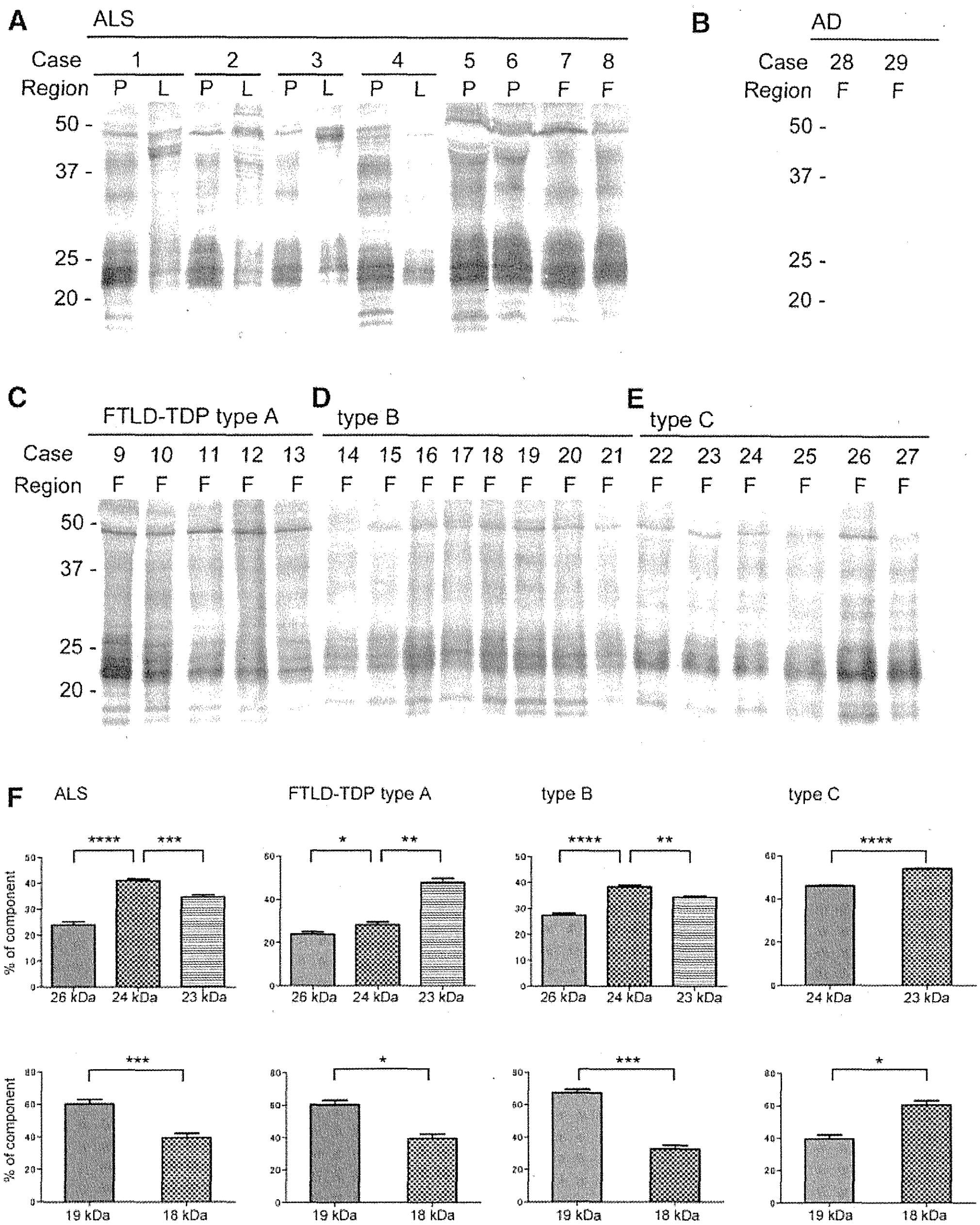

Figure 1 Immunoblot analyses of sarkosyl-insoluble TDP-43 in the brains or spinal cords of ALS (Cases 1–8) (**A**), Alzheimer's disease (Cases 28–29) (**B**), FTLD-TDP type A (Cases 9–13) (**C**), FTLD-TDP type B (Cases 14–21) (**D**) and FTLD-TDP type C (Cases 22–27) (**E**), using a phosphorylation-dependent anti-TDP-43 antibody (pS409/410). In all cases, high-molecular-weight smearing substances, phosphorylated full-length TDP-43 at 45 kDa and several C-terminal fragments at 18–26 kDa are detected. In ALS (**A**) and FTLD-TDP type B (**D**) cases, three major bands at 23, 24 and 26 kDa and two minor bands at 18 and 19 kDa are detected, whereas in the FTLD-TDP Type C (**E**) cases, two major bands at 23 and 24 and two minor bands at 18 and 19 kDa. A 24 kDa band is the most intense in ALS (**A**) and FTLD-TDP type B (**E**), whereas a 23 kDa band is the most intense in FTLD-TDP type C (**D**). The band pattern of the cases with type A (**C**) is an intermediate between FTLD-TDP type B (**D**) and FTLD-TDP type C (**E**). In spinal cords of cases with ALS, the 18 and 19 kDa bands are hardly detectable, but the same banding pattern of the 23–26 kDa bands as in precentral gyrus is detected. No such TDP-43 fragments are detected in brains of patients with Alzheimer's disease (AD) (**B**). The intensity of each C-terminal band was analysed using the ImageJ software and each component was statistically analysed by Student's *t*-test (**F**). Data indicate mean (SEM). $^{****}P < 0.0001$, $^{***}P < 0.001$, $^{**}P < 0.01$, $^{*}P < 0.05$. F = frontal cortex; L = lumbar part of spinal cord; P = precentral cortex.

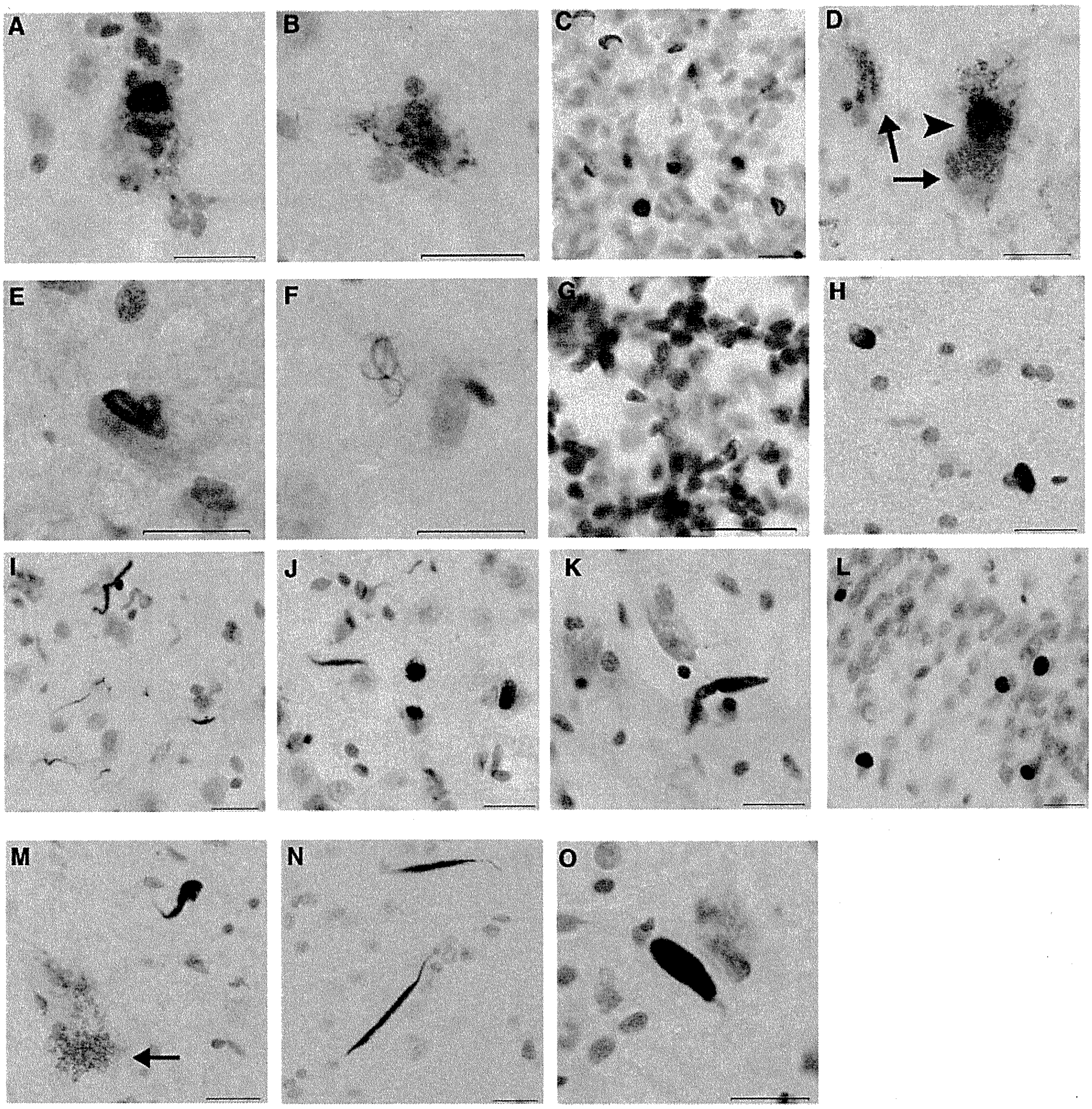

Figure 2 Phosphorylated TDP-43-positive structures observed in different brain regions and spinal cords of ALS (**A–H**) and FTLD-type C (**I–O**) using a phosphorylation-dependent anti-TDP-43 antibody (pS409/410). (**A**) Lewy body-like inclusion in the striatum neuron. (**B**) Cytoplasmic granular staining in the thalamus. (**C**) Neuronal cytoplasmic inclusions in the granular cells of hippocampus. (**D**) Irregularly shaped TDP-immunoreactive neuronal cytoplasmic inclusion in the substantia nigra (arrowhead). The arrows denote neuromelanin granules. (**E**) Skein-like inclusion in the motor nucleus of trigeminal nerve of pons. (**F**) Skein-like inclusion in the inferior olivary nucleus of medulla. (**G**) Neuronal cytoplasmic inclusion in the granular cells of cerebellar cortex. (**H**) Glial cytoplasmic inclusions in the white matter of precentral cortex. (**I**) Dystrophic neurites in the temporal cortex, (**J**) dystrophic neurites and neuronal cytoplasmic inclusions in the striatum. (**K**) Dystrophic neurites in the thalamus. (**L**) Neuronal cytoplasmic inclusions in the granular cells of hippocampus. (**M**) Dystrophic neurites in the substantia nigra. The arrow denotes neuromelanin granules. (**N**) Dystrophic neurites in the pons. (**O**) Dystrophic neurites in the medullary reticular formation. Scale bars = 20 μm.

of ALS, was detected in the temporal cortex, striatum and hippocampus, but was barely detected in the thalamus, substantia nigra, pons and medulla, and not at all in the cerebellar cortex (Fig. 3B). The banding pattern observed in these brain regions was indistinguishable (Fig. 3B). These results suggest that the same abnormal TDP-43 molecular species is deposited in different brain regions and different cell types, although the morphology of the TDP-43 inclusions may be different in the brain regions. Densitometric analyses of the immunoblots for all cases are shown in Supplementary Fig. 4.

Protease-resistant TDP-43 in ALS and FTLD with frontotemporal dementia-43 pathology

These different banding patterns in TDP-43 proteinopathies may represent different conformations of abnormal TDP-43 or their aggregates. To test this hypothesis, we subjected the abnormal TDP-43 recovered in the sarkosyl-insoluble pellets to protease treatment and analysed the protease-resistant bands. Proteins can be easily cleaved by proteases if they are denatured or unstructured, but domains that have rigid structures, such as a β-sheet conformation or that are structurally buried or interacting with other molecules, are highly resistant to proteases. On trypsin or chymotrypsin treatment, the full-length 45-kDa band and the smearing substance of TDP-43 disappeared, leaving protease-resistant fragments at 16–25 kDa (Figs 4 and 5). As expected, the protease-resistant banding patterns were different and distinguishable into three patterns (Figs 4 and 5). In ALS, trypsin-resistant doublet bands at 16 and 15 kDa, and two minor bands at ~24 kDa were detected, whereas a single band at 16 kDa and some additional bands at ~24 kDa were detected in FTLD-TDP type A (Fig. 4A, Lanes 1 and 2). In FTLD-TDP type B, the same banding pattern as that in ALS was observed (Fig. 4A, Lane 3). In FTLD-TDP type C, a broad single band at 16 kDa and some additional bands at ~24 kDa were detected (Fig. 4A, Lane 4). No such bands were detected in Alzheimer's disease (Fig. 4A, Lane 5).

Similarly, on chymotrypsin treatment, multiple protease-resistant bands were detected at 16–25 kDa and the chymotrypsin-resistant band patterns were also different between the three disease subtypes (Fig. 4B). Doublet bands were seen in ALS and FTLD-TDP type B, but only a single band in FTLD-TDP type C was detected at ~16 kDa (Fig. 4B). In FTLD-TDP type A, the lower band (15 kDa) of the ~16 kDa doublet was more intense than the upper one (16 kDa).

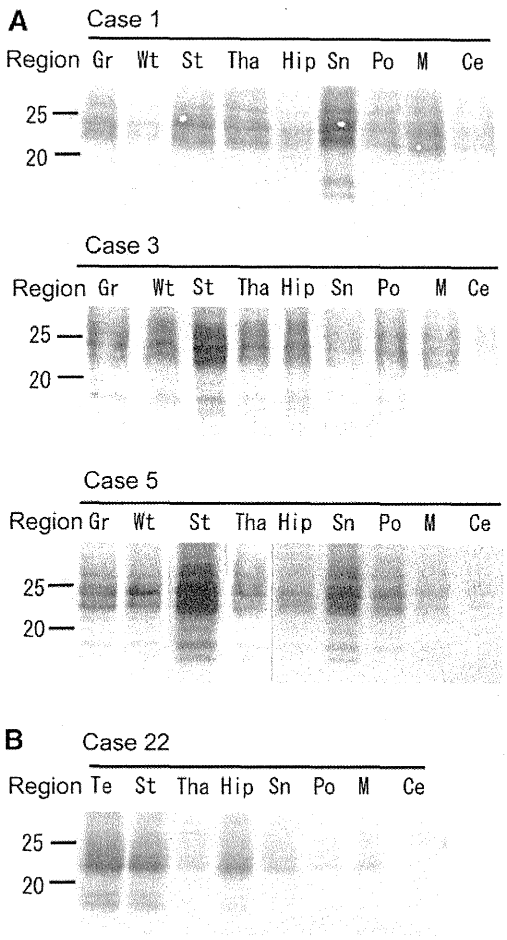

Figure 3 Immunoblot analyses of the C-terminal fragments of phosphorylated TDP-43 in the different brain regions of cases with ALS (Cases 1, 3 and 5, as shown in Fig. 1) (**A**) and FTLD-type C (Case 22, as shown in Fig. 1) (**B**). (**A**) Immunoblots of insoluble TDP-43 in the grey or white matter of precentral cortex, striatum, thalamus, hippocampus, substantia nigra, pons and medulla of ALS cases. (**B**) Immunoblot of TDP-43 in temporal cortex, striatum, hippocampus, thalamus, substantia nigra, pons and cerebellar cortex of the case with FTLD-TDP type C. Ce = Cerebellar cortex; Gr = grey matter of precentral gyrus; Hip = hippocampus; M = medulla; Po = pons; Sn = substantia nigra; St = striatum; Tha = thalamus; Te = temporal cortex; Wt = white matter of precentral gyrus. Immunoblots of spinal cords of cases with ALS are shown in Fig. 1.

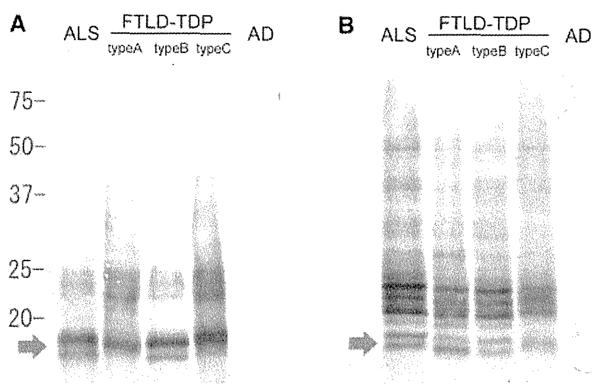

Figure 4 Immunoblot analysis of phosphorylated TDP-43 from representative ALS and FTLD-TDP cases after protease treatment. (**A**) Immunoblot of insoluble TDP-43 from cases with ALS, FTLD-TDP type A, type B, type C and Alzheimer's disease (AD) after trypsin treatment. Doublet bands at ~16 kDa (arrow) and some minor 23–24 kDa bands are detected in ALS and FTLD-TDP type B, whereas a single band at ~16 kDa and several bands at 23 and 24 kDa are detected in FTLD-TDP type A and type C. No such bands are detected in the Alzheimer's disease case. (**B**) Immunoblot of insoluble TDP-43 from cases with ALS, FTLD-TDP type A, type B, type C and Alzheimer's disease after chymotrypsin treatment. Multiple protease-resistant TDP-43 bands are detected at 16–25 kDa. Doublet bands at ~16 kD (arrow) are detected in ALS and FTLD-TDP type A and B, whereas a single band at ~16 kD (arrow) is detected in the case with FTLD-TDP type C. In FTLD-TDP type A, the lower band of the doublet at 16 kDa is more intense. No such bands are detected in the Alzheimer's disease case.

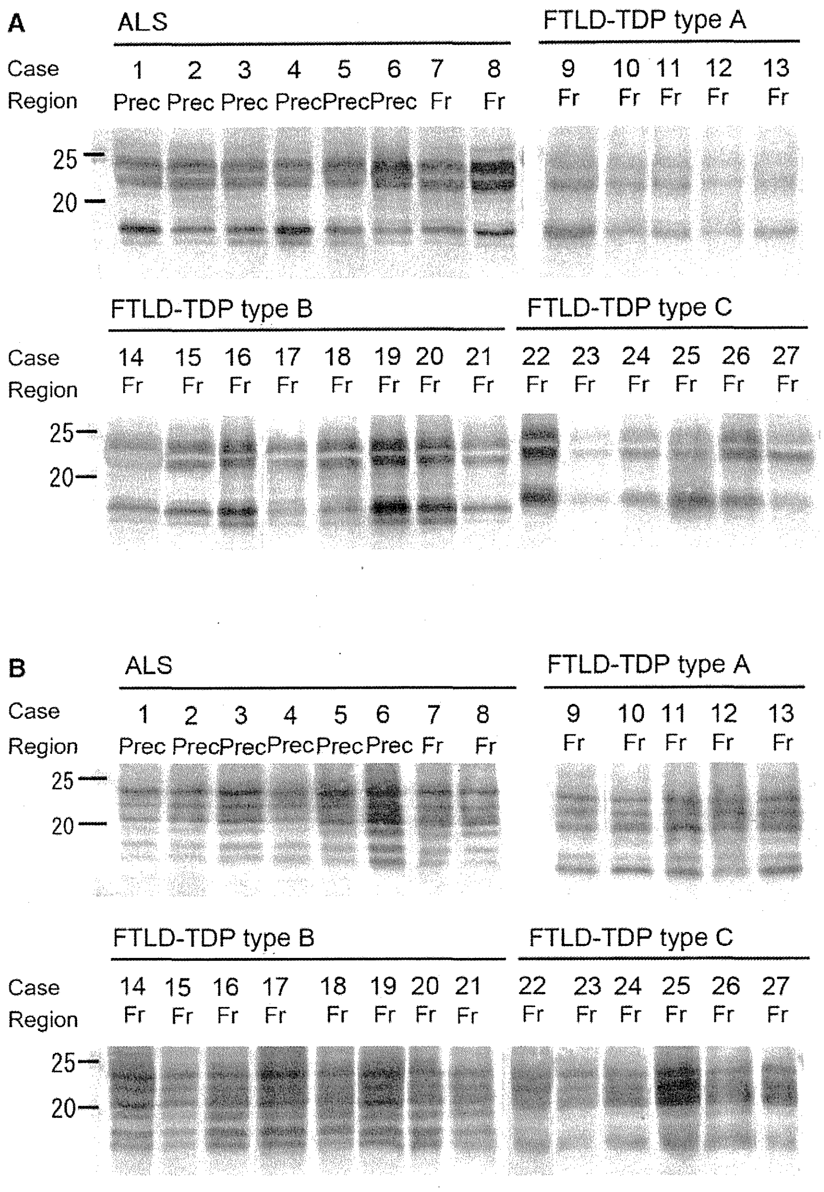

Figure 5 Comparison of the protease-resistant TDP-43 banding patterns in ALS and FTLD-TDP. Immunoblot analyses of trypsin-resistant (**A**) and chymotrypsin-resistant (**B**) fragments of TDP-43 from all cases examined. The banding patterns of ALS and FTLD-TDP type B cases are indistinguishable. Fr = frontal cortex; Prec = precentral gyrus.

In all cases examined, the trypsin-resistant banding patterns were clearly distinguishable between the disease subtypes in accordance with the three different types of banding pattern of TDP-43 C-terminal fragments, although it is difficult to distinguish the trypsin band pattern of type A from that of type C (Figs 5A, 6A and Supplementary Fig. 5). The chymotrypsin-resistant banding patterns were distinguishable and could be differentiated into three types (Figs 5B, 6B and Supplementary Fig. 6), also in accordance with the banding pattern of the TDP-43 C-terminal fragment. The banding patterns of ALS and FTLD-TDP type B were the same, whereas the banding pattern of FTLD-TDP type A was distinguishable from those of type C and type B (Figs 4 and 5). The combination analyses of trypsin and chymotrypsin-resistant banding patterns confirmed that TDP-43 proteinopathies can also be biochemically distinguishable into three types according to TDP-43 subtypes. These results strongly suggest that the different C-terminal banding patterns represent different conformations of TDP-43 aggregates and that the distinct types of TDP-43 are deposited in association with distinct pathological phenotypes of TDP-43 proteinopathies.

Immunoblot analysis using phosphorylation independent TDP-43 polyclonal and monoclonal antibodies detected some TDP-43 fragments in the ALS and FTLD-TDP cases after trypsin or chymotrypsin treatment, although no clear difference was observed in the banding patterns between ALS and other subtypes of FTLD-TDP (Supplementary Fig. 7). The distinctive

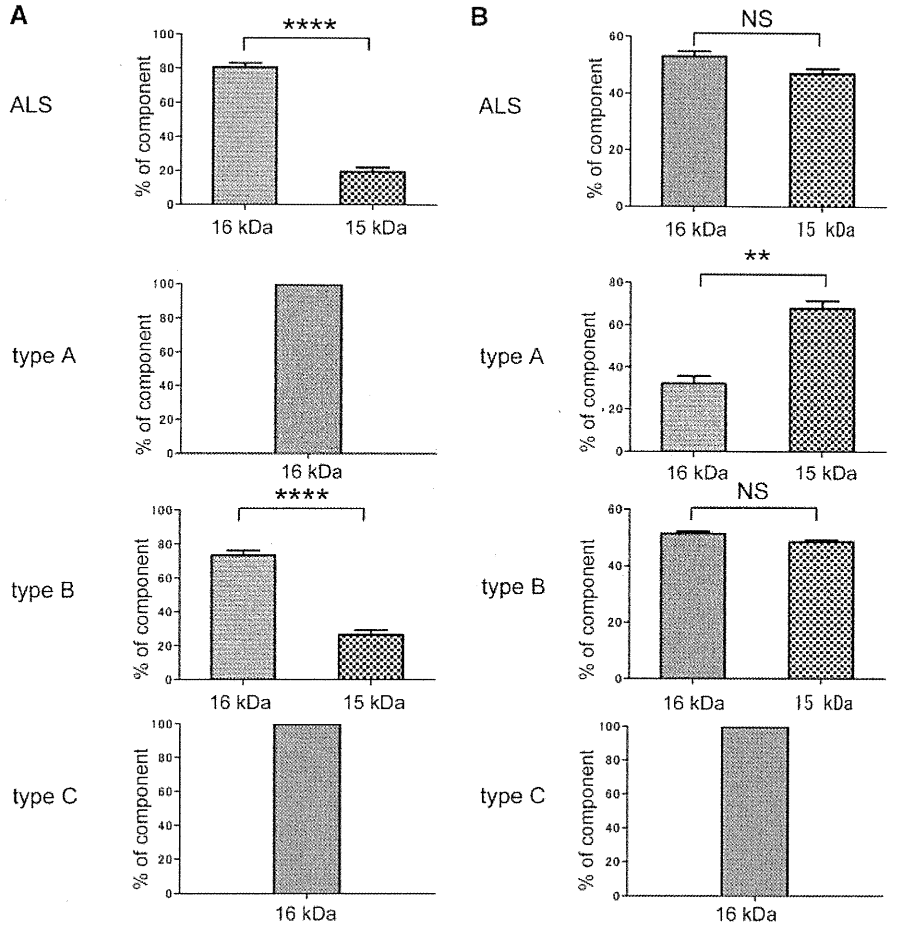

Figure 6 Quantitative analysis of protease-resistant ~16 kDa band. (**A**) The intensity of trypsin-resistant ~16 kDa band of each case was quantitated with ImageJ and statistically analysed. (**B**) The intensity of chymotrypsin-resistant ~16 kDa band of each case was quantitated with ImageJ and statistically analysed. Data indicate mean (SEM). ****$P < 0.0001$, **$P < 0.01$, NS = not significant.

protease-resistant bands at ~16 kDa of ALS were not detected with both phosphorylation independent antibodies (Supplementary Fig. 8).

We also analysed the banding pattern of phosphorylated TDP-43 in another series of five sporadic cases with TDP-43 pathology (Alzheimer's disease, Alzheimer's disease/dementia with Lewy bodies and Alzheimer's disease/argyrophilic grain disease) (Supplementary Table 1). The banding pattern of the C-terminal fragments, and trypsin- or chymotrypsin-resistant fragments, in these were same as those of FTLD-TDP type A with *GRN* mutation (Supplementary Fig. 9).

Mass spectrometric analysis of protease-resistant bands of TDP-43 in ALS and FTLD-TDP type C

To further investigate the differences in the abnormal TDP-43 protein species at a molecular level, we analysed the ~16 kDa trypsin-resistant bands by mass spectrometry. Mass analysis of chymotrypsin digests of ~16 kDa trypsin-resistant fragments identified 4 peptides, amino acid residues 277–289, 290–299, 294–333 and 300–316, suggesting these peptides are derived from trypsin-resistant fragments 276–414 and 294–414. Mass spectrometric analysis of the single broad band from FTLD-TDP type C identified the peptides of amino acids 273–283, 277–289, 290–313 and 317–330, strongly suggesting that the trypsin-resistant fragments from FTLD-TDP type C are derived from peptides 273–414 and 276–414. These analyses clearly indicate that trypsin-resistant core regions of the abnormal TDP-43 accumulated in the brain are not necessarily the same between ALS and FTLD (Supplementary Fig. 10).

Discussion

In this study, we have shown that the banding patterns for TDP-43 C-terminal fragments in ALS and FTLD are distinguishable and classifiable into at least three types. This difference was consistently demonstrated in 27 cases, eight with ALS, five with FTLD-TDP type A, eight with FTLD-TDP type B and six with FTLD-TDP type C. These results strongly suggest that distinct types of TDP-43 molecules constitute the distinct types of pathologies of TDP-43 and determine the clinicopathological phenotypes of TDP-43 proteinopathies. In TDP-43 histopathology, ALS is considered to represent a distinct pathological subtype because the distribution of TDP-43 inclusions is different from that of FTLD-TDP (Mackenzie *et al.*, 2006a). However, as shown in this study, the TDP-43 accumulations in ALS and FTLD-TDP type B are biochemically indistinguishable. In fact, clinical and histopathological motor neuron disease is often present in cases with FTLD-TDP type B histology. In the three types of phosphorylated C-terminal TDP-43 banding pattern, the pattern seen in FTLD-TDP type C is the most distinctive, lacking the 26 kDa band detected in ALS, FTLD-TDP type A and type B cases (Fig. 1). The clinical diagnosis of the FTLD-TDP type C cases was semantic dementia in every instance, consistent with other studies showing this type of histology to be associated with semantic dementia (Mackenzie *et al.*, 2006a). FTLD is clinically classified into frontotemporal dementia, demantic dementia and progressive non-fluent aphasia, based on topographical distributions of degeneration (Neary *et al.*, 1998). In frontotemporal dementia, the bilateral frontal and temporal lobes are affected, whereas the bilateral temporal lobes are affected in semantic dementia and the left hemisphere in progressive non-fluent aphasia. Present data showing the most distinctive pattern of abnormal TDP-43 in type C indicate that semantic dementia may be biochemically different from frontotemporal dementia. Similar differences in tau fragment banding patterns have been shown between progressive supranuclear palsy and corticobasal degeneration (Arai *et al.*, 2004). Progressive supranuclear palsy and corticobasal degeneration are neurodegenerative diseases that are characterized by intracytoplasmic aggregates of hyperphosphorylated tau with four microtubule-binding repeats, with distinctive pathological features. Immunoblot analysis of Sarkosyl-insoluble tau demonstrated that a 33 kDa C-terminal fragment of tau band predominated in progressive supranuclear palsy, whereas two closely related bands of ~37 kDa predominated in corticobasal degeneration. The clinicopathological subtypes of these diseases may be explained by different conformations of protein aggregates or species of abnormal proteins.

Unfortunately, we were unable to obtain brain tissue samples from patients with FTLD-TDP type D (associated with *VCP* mutation; Cairns *et al.*, 2007b; Neumann *et al.*, 2007). However, because the deposition of abnormal TDP-43 in this disorder is mostly within neuronal nuclei, it is possible that the conformation of abnormal TDP-43 in FTLD-TDP type D may also differ from that in FTLD-TDP types A–C. Familial ALS and FTLD-TDP cases in which known mutations [*GRN* (Baker *et al.*, 2006) or *C9ORF72* (DeJesus-Hernandez *et al.*, 2011; Renton *et al.*, 2011)] were examined in this study. In FTLD-TDP due to *GRN* mutations, type A pathology is exclusively seen (Mackenzie *et al.*, 2006b; Cairns *et al.*, 2007b; Josephs *et al.*, 2007). All our cases with FTLD with *GRN* mutation showed the same C-terminal banding patterns of phosphorylated TDP-43 corresponding to type A histology. Some recent studies describing the clinical and pathological features of cases of FTLD-TDP with hexanucleotide repeat expansions in *C9ORF72* reported that many of the 'pure' frontotemporal dementia cases had type A pathology, whereas many of the combined frontotemporal dementia and motor neuron disease cases had type B pathology (Murray *et al.*, 2011; Boeve *et al.*, 2012; Hsiung *et al.*, 2012; Mahoney *et al.*, 2012; Simon-Sanchez *et al.*, 2012; Snowden *et al.*, 2012). Present cases with *C9ORF72* expansions included one case of ALS, one case of pure frontotemporal dementia with type A pathology, and two cases of frontotemporal dementia with motor neuron disease and type B pathology. The C-terminal banding pattern of these cases with familial ALS and frontotemporal dementia with motor neuron disease was not different from that in the sporadic ALS and FTLD-TDP type B cases, and that of the frontotemporal dementia case was not different from that in the cases with *GRN* mutation. Therefore, expansions in *C9ORF72* do not seem to influence the various types of TDP-43 C-terminal banding pattern or histological type of TDP-43 pathology.

Immunohistochemical studies using TDP-43 antibodies have shown that pathological TDP-43 is present throughout many CNS areas in ALS, suggesting that ALS does not selectively affect only the motor system, but is rather a multisystem neurodegenerative TDP-43 proteinopathy (Geser *et al.*, 2008). We also confirmed this viewpoint, immunohistochemically and biochemically, finding the same disease characteristic C-terminal fragment (banding) patterns of phosphorylated TDP-43 within the cerebral cortex, spinal cord and the other different brain regions in ALS. Although the types of pathological structures or their morphologies detected on immunohistochemistry analysis appeared different, the banding patterns for the C-terminal fragments were the same in all regions examined in three patients with ALS. This was also true for the one case with FTLD-TDP type C, where the same banding pattern of the C-terminal fragments was detected in several different brain regions beyond the frontal cortex (Fig. 3). These results strongly suggest that the same abnormal TDP-43 molecule is deposited in different brain regions in ALS (and probably also in FTLD-TDP type B) and FTLD-TDP type C, although we need to examine whether this is also true for cases with FTLD-TDP type A. Importantly, the extent of the abnormal protein pathology is closely correlated with the disease progression, such as Alzheimer's disease in tauopathies (Braak and Braak, 1991), and Parkinson's disease in α-synucleinopathies (Braak *et al.*, 2003; Saito *et al.*, 2003). However, the molecular mechanisms governing different clinicopathological phenotypes of these neurodegenerative diseases and their progression are poorly understood. Recent studies using cellular or animal models have suggested that aggregation-prone proteins, such as tau and α-synuclein, can spread to other cells and brain regions like prion disorders (Clavaguera *et al.*, 2009; Frost *et al.*, 2009; Nonaka *et al.*, 2010). The spreading of α-synuclein lesions to the grafts is also observed in Parkinson's disease brains after transplantation (Li *et al.*, 2008). However, it remains to be clarified whether the 'propagating' abnormal protein species represents a distinct 'strain type' that can be differentiated by molecular criteria in human patients or whether the species are the same in different brain regions.

We have also shown that the banding patterns of protease-resistant fragments of phosphorylated TDP-43 are similarly different in accordance with the banding patterns seen in untreated C-terminal fragments, confirming the direct link between neuropathological subtypes and biochemical banding patterns. The mass spectrometric analysis indicated that the protease resistant regions of abnormal TDP-43 are different between the diseases. As abnormally phosphorylated TDP-43 has been shown to accumulate in a filamentous form in ALS spinal cords (Hasegawa *et al*., 2008), the filament core regions may be different between the diseases. Protease-resistant bands, and differences in banding patterns, have been reported in the prion diseases, Creutzfeldt–Jakob disease and bovine spongiform encephalopathy (Collinge *et al*., 1996). Protease-resistant prion protein extracted from cases with new-variant Creutzfeldt–Jakob disease showed a different and characteristic pattern from that in cases with sporadic Creutzfeldt–Jakob disease, with the banding pattern being indistinguishable from that of mice infected with bovine spongiform encephalopathy prion. Protease-treated prion protein species are thought to have different mobilities because of different conformations. These observations in prion disease suggest that the different banding patterns to the abnormal TDP-43 fragments in ALS and FTLD might represent different TDP-43 strains with different conformations.

Recently, TDP-43 pathology has been detected in some cases with Alzheimer's disease (Arai *et al*., 2009). We have shown here that the banding patterns of TDP-43 in cases of Alzheimer's disease with TDP-43 pathology are the same as those in FTLD-TDP type A. These novel observations suggest a biochemical commonality between FTLD and Alzheimer's disease with respect to TDP-43 pathology.

The results shown in this study also suggest a molecular basis for the clinicopathological classification of TDP-43 proteinopathies, which complements the histological classifications (Mackenzie *et al*., 2011).

Funding

This work was supported by a Grant-in-Aid for Scientific Research (A) (to M.H., 11000624) from Ministry of Education, Culture, Sports, Science and Technology of Japan, and grants from Ministry of Health, Labor and Welfare of Japan (to M.H.).

Supplementary material

Supplementary material is available at *Brain* online.

References

Arai T, Mackenzie IR, Hasegawa M, Nonoka T, Niizato K, Tsuchiya K, et al. Phosphorylated TDP-43 in Alzheimer's disease and dementia with Lewy bodies. Acta Neuropathol (Berl) 2009; 117: 125–36.

Arai T, Hasegawa M, Akiyama H, Ikeda K, Nonaka T, Mori H, et al. TDP-43 is a component of ubiquitin-positive tau-negative inclusions in frontotemporal lobar degeneration and amyotrophic lateral sclerosis. Biochem Biophys Res Commun 2006; 351: 602–11.

Arai T, Ikeda K, Akiyama H, Nonaka T, Hasegawa M, Ishiguro K, et al. Identification of amino-terminally cleaved tau fragments that distinguish progressive supranuclear palsy from corticobasal degeneration. Ann Neurol 2004; 55: 72–9.

Armstrong RA, Ellis W, Hamilton RL, Mackenzie IR, Hedreen J, Gearing M, et al. Neuropathological heterogeneity in frontotemporal lobar degeneration with TDP-43 proteinopathy: a quantitative study of 94 cases using principal components analysis. J Neural Transm 2010; 117: 227–39.

Baker M, Mackenzie IR, Pickering-Brown SM, Gass J, Rademakers R, Lindholm C, et al. Mutations in progranulin cause tau-negative frontotemporal dementia linked to chromosome 17. Nature 2006; 442: 916–19.

Boeve BF, Boylan KB, Graff-Radford NR, Dejesus-Hernandez M, Knopman DS, Pedraza O, et al. Characterization of frontotemporal dementia and/or amyotrophic lateral sclerosis associated with the GGGGCC repeat expansion in *C9ORF72*. Brain 2012; 135: 765–83.

Braak H, Braak E. Neuropathological stageing of Alzheimer-related changes. Acta Neuropathol 1991; 82: 239–59.

Braak H, Del Tredici K, Rub U, de Vos RA, Jansen Steur EN, Braak E. Staging of brain pathology related to sporadic Parkinson's disease. Neurobiol Aging 2003; 24: 197–211.

Brooks BR. El Escorial World Federation of Neurology criteria for the diagnosis of amyotrophic lateral sclerosis. Subcommittee on Motor Neuron Diseases/Amyotrophic Lateral Sclerosis of the World Federation of Neurology Research Group on Neuromuscular Diseases and the El Escorial "Clinical limits of amyotrophic lateral sclerosis" workshop contributors. J Neurol Sci 1994; 124 (Suppl): 96–107.

Cairns NJ, Bigio EH, Mackenzie IR, Neumann M, Lee VM, Hatanpaa KJ, et al. Neuropathologic diagnostic and nosologic criteria for frontotemporal lobar degeneration: consensus of the Consortium for Frontotemporal Lobar Degeneration. Acta Neuropathol 2007a; 114: 5–22.

Cairns NJ, Neumann M, Bigio EH, Holm IE, Troost D, Hatanpaa KJ, et al. TDP-43 in familial and sporadic frontotemporal lobar degeneration with ubiquitin inclusions. Am J Pathol 2007b; 171: 227–40.

Clavaguera F, Bolmont T, Crowther RA, Abramowski D, Frank S, Probst A, et al. Transmission and spreading of tauopathy in transgenic mouse brain. Nat Cell Biol 2009; 11: 909–13.

Collinge J, Sidle KC, Meads J, Ironside J, Hill AF. Molecular analysis of prion strain variation and the aetiology of 'new variant' CJD. Nature 1996; 383: 685–90.

DeJesus-Hernandez M, Mackenzie IR, Boeve BF, Boxer AL, Baker M, Rutherford NJ, et al. Expanded GGGGCC hexanucleotide repeat in noncoding region of *C9ORF72* causes chromosome 9p-linked FTD and ALS. Neuron 2011; 72: 245–56.

Frost B, Jacks RL, Diamond MI. Propagation of tau misfolding from the outside to the inside of a cell. J Biol Chem 2009; 284: 12845–52.

Geser F, Brandmeir NJ, Kwong LK, Martinez-Lage M, Elman L, McCluskey L, et al. Evidence of multisystem disorder in whole-brain map of pathological TDP-43 in amyotrophic lateral sclerosis. Arch Neurol 2008; 65: 636–41.

Geser F, Martinez-Lage M, Robinson J, Uryu K, Neumann M, Brandmeir NJ, et al. Clinical and pathological continuum of multisystem TDP-43 proteinopathies. Arch Neurol 2009; 66: 180–9.

Gitcho MA, Bigio EH, Mishra M, Johnson N, Weintraub S, Mesulam M, et al. TARDBP 3'-UTR variant in autopsy-confirmed frontotemporal lobar degeneration with TDP-43 proteinopathy. Acta Neuropathol 2009; 118: 633–45.

Hasegawa M, Arai T, Nonaka T, Kametani F, Yoshida M, Hashizume Y, et al. Phosphorylated TDP-43 in frontotemporal lobar degeneration and amyotrophic lateral sclerosis. Ann Neurol 2008; 64: 60–70.

Hsiung GY, Dejesus-Hernandez M, Feldman HH, Sengdy P, Bouchard-Kerr P, Dwosh E, et al. Clinical and pathological features of familial frontotemporal dementia caused by *C9ORF72* mutation on chromosome 9p. Brain 2012; 135: 709–22.

Inukai Y, Nonaka T, Arai T, Yoshida M, Hashizume Y, Beach TG, et al. Abnormal phosphorylation of Ser409/410 of TDP-43 in FTLD-U and ALS. FEBS Lett 2008; 582: 2899–904.

Josephs KA, Ahmed Z, Katsuse O, Parisi JF, Boeve BF, Knopman DS, et al. Neuropathologic features of frontotemporal lobar degeneration with ubiquitin-positive inclusions with progranulin gene (*GRN*) mutations. J Neuropathol Exp Neurol 2007; 66: 142–51.

Kabashi E, Valdmanis PN, Dion P, Spiegelman D, McConkey BJ, Vande Velde C, et al. TARDBP mutations in individuals with sporadic and familial amyotrophic lateral sclerosis. Nat Genet 2008; 40: 572–4.

Kovacs GG, Murrell JR, Horvath S, Haraszti L, Majtenyi K, Molnar MJ, et al. TARDBP variation associated with frontotemporal dementia, supranuclear gaze palsy, and chorea. Mov Disord 2009; 24: 1843–7.

Li JY, Englund E, Holton JL, Soulet D, Hagell P, Lees AJ, et al. Lewy bodies in grafted neurons in subjects with Parkinson's disease suggest host-to-graft disease propagation. Nat Med 2008; 14: 501–3.

Mackenzie IR, Baborie A, Pickering-Brown S, Du Plessis D, Jaros E, Perry RH, et al. Heterogeneity of ubiquitin pathology in frontotemporal lobar degeneration: classification and relation to clinical phenotype. Acta Neuropathol 2006a; 112: 539–49.

Mackenzie IR, Baker M, Pickering-Brown S, Hsiung GY, Lindholm C, Dwosh E, et al. The neuropathology of frontotemporal lobar degeneration caused by mutations in the progranulin gene. Brain 2006b; 129: 3081–90.

Mackenzie IR, Neumann M, Baborie A, Sampathu DM, Du Plessis D, Jaros E, et al. A harmonized classification system for FTLD-TDP pathology. Acta Neuropathol 2011; 122: 111–13.

Mahoney CJ, Beck J, Rohrer JD, Lashley T, Mok K, Shakespeare T, et al. Frontotemporal dementia with the *C9ORF72* hexanucleotide repeat expansion: clinical, neuroanatomical and neuropathological features. Brain 2012; 135: 736–50.

Murray ME, DeJesus-Hernandez M, Rutherford NJ, Baker M, Duara R, Graff-Radford NR, et al. Clinical and neuropathologic heterogeneity of c9FTD/ALS associated with hexanucleotide repeat expansion in *C9ORF72*. Acta Neuropathol 2011; 122: 673–90.

Neary D, Snowden JS, Gustafson L, Passant U, Stuss D, Black S, et al. Frontotemporal lobar degeneration: a consensus on clinical diagnostic criteria. Neurology 1998; 51: 1546–54.

Neumann M, Mackenzie IR, Cairns NJ, Boyer PJ, Markesbery WR, Smith CD, et al. TDP-43 in the ubiquitin pathology of frontotemporal dementia with *VCP* gene mutations. J Neuropathol Exp Neurol 2007; 66: 152–7.

Neumann M, Sampathu DM, Kwong LK, Truax AC, Micsenyi MC, Chou TT, et al. Ubiquitinated TDP-43 in frontotemporal lobar degeneration and amyotrophic lateral sclerosis. Science 2006; 314: 130–3.

Nonaka T, Watanabe ST, Iwatsubo T, Hasegawa M. Seeded aggregation and toxicity of α-synuclein and tau: cellular models of neurodegenerative diseases. J Biol Chem 2010; 285: 34885–98.

Renton AE, Majounie E, Waite A, Simon-Sanchez J, Rollinson S, Gibbs JR, et al. A hexanucleotide repeat expansion in *C9ORF72* is the cause of chromosome 9p21-linked ALS-FTD. Neuron 2011; 72: 257–68.

Saito Y, Kawashima A, Ruberu NN, Fujiwara H, Koyama S, Sawabe M, et al. Accumulation of phosphorylated alpha-synuclein in aging human brain. J Neuropathol Exp Neurol 2003; 62: 644–54.

Simon-Sanchez J, Dopper EG, Cohn-Hokke PE, Hukema RK, Nicolaou N, Seelaar H, et al. The clinical and pathological phenotype of *C9ORF72* hexanucleotide repeat expansions. Brain 2012; 135: 723–35.

Snowden JS, Rollinson S, Thompson JC, Harris JM, Stopford CL, Richardson AM, et al. Distinct clinical and pathological characteristics of frontotemporal dementia associated with *C9ORF72* mutations. Brain 2012; 135: 693–708.

Sreedharan J, Blair IP, Tripathi VB, Hu X, Vance C, Rogelj B, et al. TDP-43 mutations in familial and sporadic amyotrophic lateral sclerosis. Science 2008; 319: 1668–72.

Tan CF, Eguchi H, Tagawa A, Onodera O, Iwasaki T, Tsujino A, et al. TDP-43 immunoreactivity in neuronal inclusions in familial amyotrophic lateral sclerosis with or without SOD1 gene mutation. Acta Neuropathol 2007; 113: 535–42.

Biochemical and Biophysical Research Communications 417 (2012) 116–121

Contents lists available at SciVerse ScienceDirect

Biochemical and Biophysical Research Communications

journal homepage: www.elsevier.com/locate/ybbrc

Epitope mapping of antibodies against TDP-43 and detection of protease-resistant fragments of pathological TDP-43 in amyotrophic lateral sclerosis and frontotemporal lobar degeneration

Hiroshi Tsuji [a,b], Takashi Nonaka [a], Makiko Yamashita [a], Masami Masuda-Suzukake [a], Fuyuki Kametani [a], Haruhiko Akiyama [c], David M.A. Mann [d], Akira Tamaoka [b], Masato Hasegawa [a,*]

[a] Department of Neuropathology and Cell Biology, Tokyo Metropolitan Institute of Medical Science, 2-1-6 Kamikitazawa, Setagaya-ku, Tokyo 156-8506, Japan
[b] Department of Neurology, Graduate School of Comprehensive Human Sciences, University of Tsukuba, 1-1-1 Tenodai, Tsukuba-City, Ibaraki 305-8576, Japan
[c] Dementia Research Project, Tokyo Metropolitan Institute of Medical Science, 2-1-6 Kamikitazawa, Setagaya-ku, Tokyo 156-0057, Japan
[d] Mental Health and Neurodegeneration Research Group, Greater Manchester Neuroscience Centre, University of Manchester, Hope Hospital, Salford M6 8HD, UK

ARTICLE INFO

Article history:
Received 8 November 2011
Available online 22 November 2011

Keywords:
Aggregation
Tau
Alpha-synuclein
ALS
FTLD

ABSTRACT

TAR DNA-binding protein of 43 kDa (TDP-43) is the major component of the intracellular inclusions in amyotrophic lateral sclerosis (ALS) and frontotemporal lobar degeneration (FTLD). Here, we show that both monoclonal (60019-2-Ig) and polyclonal (10782-2-AP) anti-TDP-43 antibodies recognize amino acids 203–209 of human TDP-43. The monoclonal antibody labeled human TDP-43 by recognizing Glu204, Asp205 and Arg208, but failed to react with mouse TDP-43. The antibodies stained the abnormally phosphorylated C-terminal fragments of 24–26 kDa in addition to normal TDP-43 in ALS and FTLD brains. Immunoblot analysis after protease treatment demonstrated that the epitope of the antibodies (residues 203–209) constitutes part of the protease-resistant domain of TDP-43 aggregates which determine a common characteristic of the pathological TDP-43 in both ALS and FTLD-TDP. The antibodies and methods used in this study will be useful for the characterization of abnormal TDP-43 in human materials, as well as in vitro and animal models for TDP-43 proteinopathies.

1. Introduction

TDP-43 is a nuclear ribonucleoprotein implicated in exon splicing, gene transcription, regulation of mRNA stability, mRNA biosynthesis, and formation of nuclear bodies [1–5]. It has been identified as the major component of the ubiquitin-positive tau-negative intracytoplasmic inclusions in frontotemporal lobar degeneration (FTLD), amyotrophic lateral sclerosis (ALS) [6,7] and other neurodegenerative disorders [8–12]. Identification of mutations in familial and sporadic ALS and FTLD cases demonstrated a direct link between the genetic lesion and development of TDP-43 pathology [13–16]. Immunohistochemical studies using anti-TDP-43 antibodies revealed that TDP-43 translocates from its normal nuclear localization into the cytoplasm in these disorders. Furthermore, biochemical analysis detected abnormally phosphorylated TDP-43 of 45 kDa, high-molecular-weight smearing and C-terminal fragments of approximately 25 kDa, as well as normal TDP-43 of 43 kDa in the detergent-insoluble, urea-soluble fraction from affected brains. The antibodies generated by immunizing C-terminal phosphopeptides of TDP-43, such as pS409/410 and pS403/404, strongly stain abnormal neuronal cytoplasmic and dendritic inclusions in FTLD, and skein-like and glial cytoplasmic inclusions in ALS spinal cord, with no nuclear staining, and thus permit easier and more sensitive detection of abnormal TDP-43 accumulations in neuropathological examination [17]. Immunoblotting of the Sarkosyl-insoluble fractions from FTLD and ALS cases using these phosphospecific antibodies clearly demonstrated that hyperphosphorylated full-length TDP-43 of 45 kDa, smearing substances and fragments at 18–26 kDa are the major species of TDP-43 accumulated in FTLD and ALS, and the band patterns of the C-terminal fragments of phosphorylated TDP-43 correspond to the neuropathological subtypes.

Anti-TDP-43 monoclonal antibody (mAb) (60019-2-Ig; Proteintech Group Inc., Chicago, IL) and polyclonal antibody (pAb) (10782-2-AP; Proteintech Group Inc., Chicago, IL) are widely used for the investigation of TDP-43 pathology [6,7,9,18–21]. According to the manufacturer's specifications, anti-TDP-43 mAb and pAb were generated against the N-terminal 260 amino acids (aa) of the protein, but the precise epitope has not yet been identified. Another mouse monoclonal antibody against TDP-43 (2E2-D3; Abnova Corporation, Taipei, Taiwan) is also commercially available; it recognizes residues 205–222 of human TDP-43, but does not recognize mouse or rat TDP-43 [22].

* Corresponding author. Fax: +81 3 6834 2349.
E-mail address: hasegawa-ms@igakuken.or.jp (M. Hasegawa).

0006-291X/$ - see front matter © 2011 Elsevier Inc. All rights reserved.
doi:10.1016/j.bbrc.2011.11.066

In this study, we mapped the epitope for anti-TDP-43 mAb and pAb (Proteintech Group Inc.). We also showed that anti-TDP-43 mAb recognizes human TDP-43, but not mouse TDP-43. Using these antibodies, we investigated the abnormal forms of TDP-43 from ALS and FTLD brains, and found that the antibodies recognized the amino-terminus of the TDP-43 C-terminal fragments of 24–26 kDa. Immunoblot analysis of Sarkosyl-insoluble fractions after treatment of proteases also demonstrated that the epitope is apparently resistant to trypsin and chymotrypsin in the abnormal TDP-43, suggesting that the epitope region is important for the formation of the pathological structure of TDP-43 in ALS and FTLD.

Table 1
Description of subjects.

Case No.	Diagnosis	Age (years)	Sex	BW (g)
1	AD	65	F	1165
2	AD	70	F	1126
3	ALS	62	M	1230
4	ALS	42	F	1140
5	FTLD-TDP (type A)	71	F	863
6	FTLD-TDP (type A)	66	F	1100
7	FTLD-TDP (type B)	45	M	1260
8	FTLD-TDP (type B)	67	M	1280
9	FTLD-TDP (type C)	67	M	na
10	FTLD-TDP (type C)	59	M	na

BW, brain weight; AD, Alzheimer's disease; ALS, amyotrophic lateral sclerosis; FTLD-TDP, frontotemporal lobar degeneration with TDP-43 pathology; na, not available.

2. Materials and methods

2.1. Construction of plasmids

GFP-tagged TDP-43 C-terminal or N-terminal fragments were constructed as described [23] by amplifying a cDNA encoding full-length TDP-43 by means of PCR and inserting the fragment into the pEGFP-C1 vector (Clontech). To investigate the specificity of TDP-43 mAb for human TDP-43, site-directed mutagenesis of GFP-tagged full-length TDP-43 was carried out to substitute Glu204 to Ala (E204A), Asp205 to Glu (D205E), Arg208 to Gln (R208Q), Glu209 to Gln (E209Q), Ser212 to Cys (S212C), Asp216 to Glu (D216E), and Met218 to Val (M218V), using a site-directed mutagenesis kit (Strategene)(Fig. 4). All constructs were verified by DNA sequencing.

2.2. Antibodies

TDP-43 polyclonal antibody, 10782-2-AP, and TDP-43 monoclonal antibody, 60019-2-Ig, were purchased from Proteintech Group Inc. Anti-GFP monoclonal antibody was purchased from MBL (Nagoya, Japan). A polyclonal antibody specific for phosphorylated TDP-43 (pS409/410) was prepared as described [17].

2.3. Cell culture and expression of plasmids

Human neuroblastoma cell line SH-SY5Y and mouse neuroblastoma cell line Neuro 2a were maintained in appropriate medium as described previously [24,25]. Cells were then transfected with expression plasmids using FuGENE6 (Roche) according to the manufacturer's instructions.

2.4. Immunoblotting

Expressed proteins in cell lysates were separated by 10% SDS–PAGE and transferred onto polyvinylidene difluoride membrane (Millipore, Bedford, MA). After blocking with 3% gelatin, membranes were incubated overnight with primary antibodies (1:1000) at room temperature. After incubation with an appropriate biotinylated secondary antibody, labeling was detected using the ABC system (Vector Lab., Burlingame, CA) coupled with a diaminobenzidine (DAB) reaction intensified with nickel chloride.

2.5. Analysis of abnormal TDP-43 in ALS and FTLD-TDP brain

Brains from two cases with Alzheimer's disease (AD), two with ALS, two with FTLD-TDP (type A), two with FTLD-TDP (type B) and two with FTLD-TDP (type C) were employed in this study. The two AD cases had no TDP-43 pathology. The age, sex, brain weight, and diagnosis are given in Table 1. Sarkosyl-insoluble, urea-soluble fractions were extracted from these brains as previously described [6,9]. The samples were loaded onto 15% polyacrylamide gel and transferred onto a membrane. The membrane was cut in the center of the loaded lane, and the same samples were reacted separately with anti-TDP-43 Abs and pS409/410 as described above.

2.6. Protease treatment of TDP-43

Sarkosyl-insoluble fractions extracted from neocortical regions of the brains were treated with trypsin (at a final concentration of 100 μg/ml, Promega, Madison, USA) or chymotrypsin (at a concentration of 10 μg/ml, Sigma–Aldrich, St. Louis, USA) at 37 °C for 30 min. The reaction was stopped by boiling for 5 min. After centrifuging at 15,000 rpm for 1 min, the samples were analyzed by immunoblotting with anti-TDP-43 pAb and mAb as described above.

3. Results

3.1. Epitope mapping of anti-TDP-43 antibody

Our previous study showed that both TDP-43 mAb and pAb reacted with GFP-tagged TDP-43 C-terminal fragment (GFP-TDP 162–414), but failed to detect GFP-TDP 218–414 [23]. To map the epitope of these antibodies, we expressed a series of GFP-tagged human TDP-43 C-terminal fragments (Fig. 1A) in SH-SY5Y cells and immunoblotted them with the antibodies. Both anti-TDP-43 pAb and mAb detected endogenous human TDP-43 of 43 kDa and exogenous GFP-tagged full-length, 171–414, 181–414, 191–414 and 201–414 TDP-43. However, both antibodies failed to detect 211–414 (Fig. 1A). These results suggest that the epitopes of these antibodies are located within residues 201–210.

To narrow down the epitope structure further, another series of GFP-tagged C-terminal fragments of TDP-43 was expressed in SH-SY5Y cells (Fig. 1B) and tested. Both antibodies reacted with GFP-TDP 203–414, but failed to recognize GFP-TDP 204–414, 205–414 and 207–414 (Fig. 1B), demonstrating that Thr203 forms the N-terminal border of the epitope for both antibodies.

To determine the C-terminus of the epitope, a series of GFP-tagged N-terminal fragments of TDP-43 was expressed and immunoblotted with these antibodies (Fig 1C). Anti-TDP-43 pAb reacted with all of the N-terminal fragments tested, although it stained the 1-212 fragment most strongly. This suggests that one of the pAb epitopes is located at the N-terminal region of TDP-43, in addition to the central epitope. Anti-TDP-43 mAb strongly stained GFP-TDP 1-212, moderately stained GFP-TDP 1-210, and barely stained GFP-TDP 1-209, while it failed to react with GFP 1-208 and 1-207 (Fig. 1C), indicating that Glu209 forms the C-terminus of the epitope for anti-TDP-43 mAb. Thus, anti-TDP-43 mAb recognizes residues 203–209 of human TDP-43.

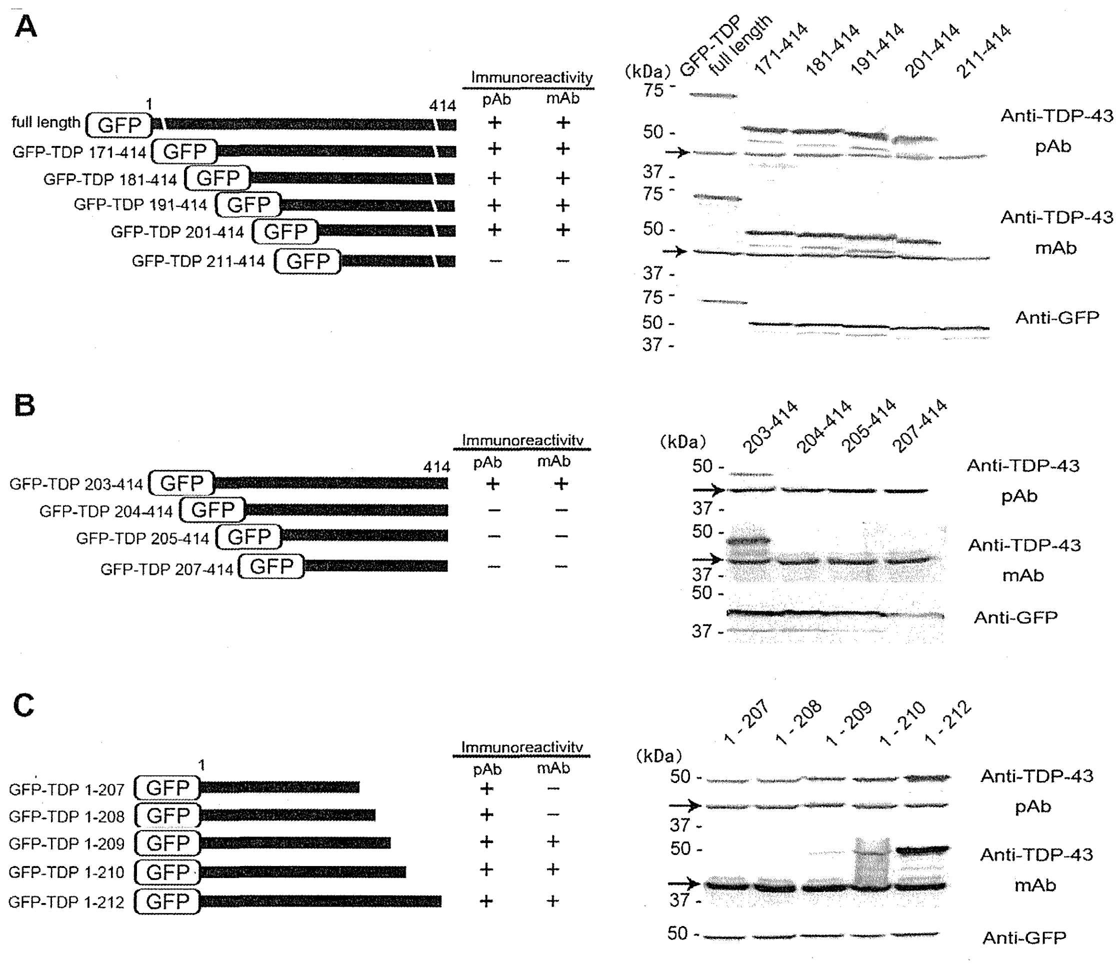

Fig. 1. Epitope mapping of anti-TDP-43 polyclonal and monoclonal antibodies. (A) Schematic diagram of GFP-tagged full-length TDP-43 (GFP-TDP) and the C-terminal fragments. Immunoblot analyses of GFP-TDP and the C-terminal fragments in SH-SY5Y cells. Both mAb and pAb reacted with GFP-TDP and the C-terminal fragments, except for 211–414. The anti-GFP antibody recognizes all the proteins expressed. (B) Further epitope mapping of anti-TDP-43 antibodies. Immunoblot analyses of the GFP tagged C-terminal fragments of TDP-43. Both mAb and pAb reacted with 203–414, but failed to recognize 204–414, 205–414, and 207–414. The anti-GFP antibody recognizes all of the fragments. (C) Epitope mapping of the C-terminus recognized by anti-TDP-43 polyclonal and monoclonal antibodies. Immunoblot analyses of GFP-TDP and N-terminal fragments in SH-SY5Y cells. Anti-TDP-43 pAb reacted with all of the N-terminal fragments, although it stained 1-212 fragment most strongly. In contrast, anti-TDP-43 mAb strongly stained GFP-TDP 1-212, moderately stained GFP-TDP 1-210, and barely stained GFP-TDP 1-209, while it failed to react with GFP 1-208 and 1-207. The anti-GFP antibody recognized all of the fragments equally. The arrows indicate endogenous TDP-43 in SH-SY5Y cells.

3.2. Amino acid sequence differences between human and mouse TDP-43

The anti-TDP-43 mAb reacted with endogenous TDP-43 of human neuroblastoma SH-SY5Y cells, but not with TDP-43 of mouse neuroblastoma Neuro2a cells (Fig. 1B, 1C, 2B). Similarly, the mAb recognized TDP-43 in human brain extract, but failed to detect TDP-43 in mouse brain extract, suggesting that the mAb does not recognize mouse TDP-43 (data not shown). The absence of reactivity with mouse TDP-43 is explained by the sequence differences around the epitope between human and mouse TDP-43 (Fig. 2A). Each different amino acid of human TDP-43 was substituted to that of mouse TDP-43. The mutated proteins were expressed in Neuro2a cells and immunoreactivity with anti-TDP-43 mAb was examined. Substitution of D216 to E and M218 to V did not affect the immunoreactivity (Fig. 2B), whereas substitutions of E204 to A, D205 to E, and R208 to Q abolished the immunoreactivity of anti-TDP-43 mAb, indicating that these residues are necessary for recognition by the mAb. Anti-TDP-43 pAb reacted with these mutants, although a marked decrease in immunoreactivity was observed in the cases of E204A, D205A, R208Q, and S212C.

3.3. Biochemical analysis of abnormal TDP-43 in ALS and FTLD brains with anti-TDP-43 mAb

On immunoblots of Sarkosyl-insoluble fractions extracted from the brain of patients with ALS and FTLD-TDP (type A), the anti-TDP-43 mAb detected phosphorylated full-length TDP-43 at 45 kDa, two bands around 25 kDa and high-molecular-weight smears, in addition to the normal TDP-43 band at 43 kDa, which can also be detected in control cases. Immunoblot analysis of the split membrane with a phosphorylation-dependent anti-TDP-43 antibody pS409/410 revealed that the two bands around 25 kDa stained with the mAb corresponded to the C-terminal fragments of 24 and 26 kDa recognized by pS409/410 (Fig. 3)[17]. These results demonstrated that these 24 and 26 kDa C-terminal fragments contain the epitope of the mAb, residues 203–209, and that the cleavage sites of these C-terminal fragments are located at the N-terminal side of Thr203.

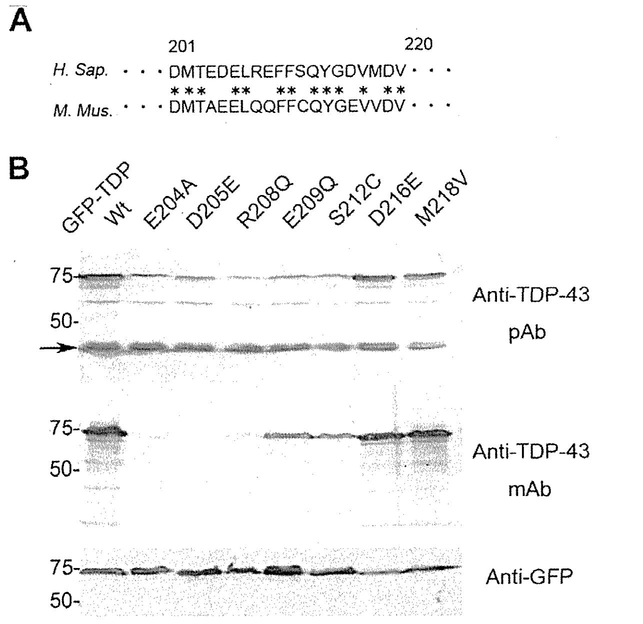

Fig. 2. Alignment of human and mouse TDP-43 (A) and immunoblot analyses of mutated TDP-43 with anti-TDP-43 antibodies. (A) The amino acid sequences of human (upper) and mouse (lower) TDP-43 around the epitope of anti-TDP-43 mAb. The asterisks show identical amino acids. (B) Immunoblot analyses of GFP-TDP wild type (Wt) and GFP-TDP mutants expressed in Neuro2a cells. Substitution of D216 to E and M218 to V did not affect the immunoreactivity, whereas substitutions of E204 to A, D205 to E, and R208 to Q, abolished the immunoreactivity of anti-TDP-43 mAb. Anti-TDP-43 pAb reacted with all these mutants, although markedly decreased immunoreactivities were observed in E204A, D205A, R208Q, and S212C. The arrows indicated endogenous TDP-43 in Neuro2A cells. Note that endogenous mouse TDP-43 in Neuro 2a cells was not recognized by anti-TDP-43 mAb.

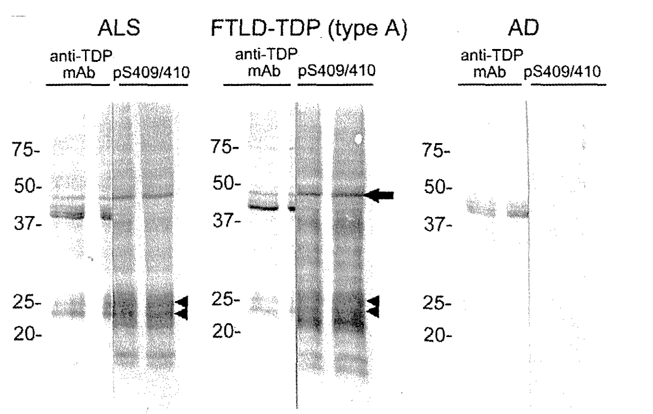

Fig. 3. Immunoblot analyses of Sarkosyl-insoluble fractions from ALS, FTLD-TDP (type A), and AD brains with anti-TDP-43 monoclonal antibody and phosphorylation-dependent anti-TDP-43 antibody, pS409/410. With pS409/410, fragments of approximately 45 kDa and 18–26 kDa, as well as smearing, were detected. The banding pattern of 18–26 kDa fragments showed three major bands at 23, 24, and 26 kDa, and 2 minor bands at 18 and 19 kDa, with the 24 kDa band being the most intense. In addition to the normal full-length TDP-43 at 43 kDa, anti-TDP-43 mAb labeled phosphorylated full-length TDP-43 at 45 kDa, high-molecular-weight smears and two bands at 26 kDa and 24 kDa (arrowheads), which were not seen in the AD case. The two bands corresponded to the major 26 and 24 kDa bands were detected with pS409/410.

3.4. The epitope of these TDP-43 antibodies constitute part of protease-resistant core domain of TDP-43 in ALS and FTLD brains

In order to characterize the epitope further, we treated the Sarkosyl-insoluble fractions extracted from brains of patients with proteases and analyzed them with these antibodies. Without protease treatment, both antibodies strongly stained normal full-length TDP-43 of 43 kDa in all cases examined including AD cases which were without TDP-43 pathology. In ALS and FTLD-TDP cases, phosphorylated full-length TDP-43 of 45 kDa (Fig 4A, arrows) and the ~25 kDa fragments (Fig 4A, arrow heads) were detected with these antibodies. After trypsin treatment, the full-length band of TDP-43 was disappeared and the protease-resistant fragments around 25 kDa (Fig 4B, white arrows) and smearing substances appeared in the ALS and FTLD-TDP cases. Similarly, after chymotrypsin treatment, protease-resistant triplet bands of 16, 20 and 25 kDa (Fig 4C, white arrow heads) and smearing substances were clearly detected in ALS and FTLD-TDP-cases with the mAb, while no such bands were seen in AD cases. On blot with the pAb, multiple bands were detected in addition to the triplet, and some of these bands were also detected in AD cases, suggesting that the pAb stained some normal fragments in addition to the abnormal TDP-43 bands. In the cases examined, apparent difference was not detected in these trypsin-resistant and chymotrypsin-resistant bands detected among the clinicopathological phenotypes of the diseases. By proteinase K treatment, immunoreactivities with these antibodies were completely abolished (data not shown), suggesting that the epitope is not entirely resistant to any proteases. However, it is obvious that the epitope of the TDP-43 deposited in the patients is fairly protease-resistant compared to the normal protein. These results indicate that the epitope of the mAb (residues 203–209 of TDP-43) constitute part of the protease-resistant domain of TDP-43 which determine a common characteristic of the abnormal TDP-43 in both ALS and FTLD-TDP.

4. Discussion

This is the first analysis of the epitopes of Proteintech's anti-TDP-43 polyclonal and monoclonal antibodies, which have often been used to research TDP-43 proteinopathies since 2006 [6,7]. We demonstrated that anti-TDP-43 mAb specifically recognizes residues 203–209 of human TDP-43, which form a part of the second RNA-recognition motif (RRM2, residues 193–257) of normal TDP-43 [26], but constitute part of the protease-resistant core domain of TDP-43 aggregates that determine the common characteristic of abnormal TDP-43 in ALS and FTLD-TDP-43.

RRM2 is a functional domain with distinct RNA/DNA binding characteristics. The anti-TDP-43 mAb recognized human TDP-43, but not mouse TDP-43. Site-directed mutagenesis and subsequent immunoblot analysis revealed that Glu204, Asp205 and Arg208 residues in human TDP-43 are important for the specific recognition by the mAb (Fig. 2). In fact, human TDP-43 shares 98.5% homology with mouse TDP-43 at the amino acid level, but the RRM2 domain has only 66% homology.

We also showed that one of the major epitopes of the pAb is located in almost the same region at that of the mAb (Fig. 1), although the pAb also recognizes the N-terminal region of TDP-43. Recently, TDP-43 transgenic mice overexpressing human TDP-43 have been produced as animal models of TDP-43 proteinopathy [27]. However, abnormal TDP-43 pathologies in these mice are very rare, so new transgenic or other animal models that develop abundant TDP-43 pathology are still required. Since the TDP-43 mAb recognizes human TDP-43, but not mouse TDP-43, it will be a useful reagent for the characterization of mouse lines transgenic for human TDP-43, together with phosphorylation-dependent antibodies.

Biochemical analyses of TDP-43 proteinopathies have demonstrated that abnormally phosphorylated full-length and C-terminal fragments of TDP-43 are the major species in the inclusions. The band patterns of the C-terminal fragments at 18–26 kDa are closely correlated with the clinicopathological subtypes of TDP-43 proteinopathies [17]. In addition, most of the pathogenic mutations

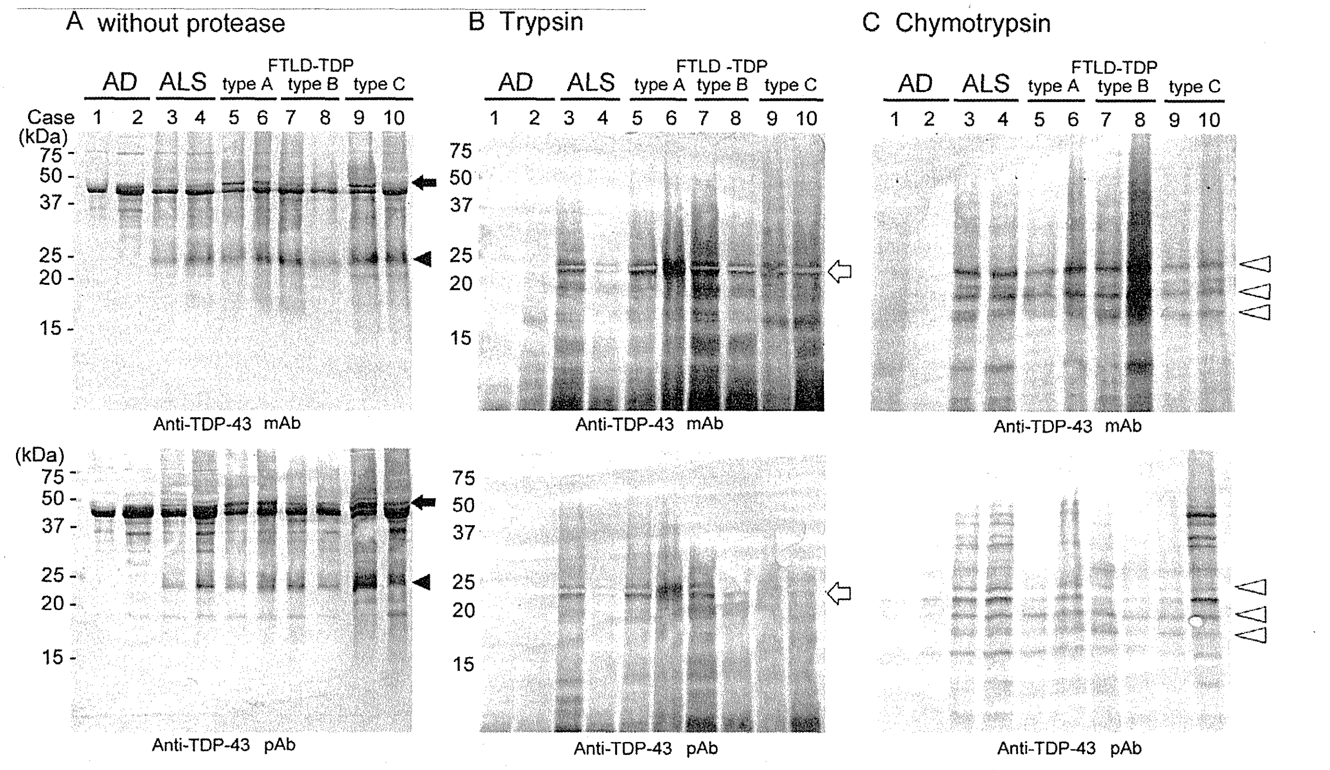

Fig. 4. Immunoblot analysis of Sarkosyl-insoluble fractions from AD and TDP-43 proteinopathies before and after protease treatment. (A) Without protease treatment, normal TDP-43 of 43 kDa was detected with these antibodies in all cases examined. In the ALS and FTLD-TDP cases, phosphorylated full-length TDP-43 of 45 kDa (arrows), high-molecular-weight smears, and the 24–26 kDa fragments (arrow heads) were detected in addition to the normal TDP-43. (B) Upon trypsin treatment, full-length TDP-43 disappeared, and the protease-resistant ~25 kDa fragments (white arrows) and smears appeared in ALS and FTLD-TDP cases, but not in AD cases. (C) After chymotrypsin treatment, triplet bands (white arrowheads) were detected in ALS and FTLD-TDP cases with the mAb and multiple bands were detected with pAb, whereas such immunoreactivities were hardly detected in AD cases.

are found in the C-terminal half of the TDP-43 [13–16]. Therefore, misfolding or structural alteration of the C-terminal half of TDP-43 seems to be the key to the pathogenesis of TDP-43 proteinopathies. By mass spectrometric analysis of the 23 kDa band in Sarkosyl-insoluble fraction from FTLD-TDP (type A), we identified the cleavage site as the N-terminus of Asp219 [23]. Another group reported cleavage at Asp208, based on N-terminal sequencing of urea extracts of FTLD-TDP brain [28]. However, the cleavage sites of the other major C-terminal fragments of 24 and 26 kDa have not been determined yet. In this study, we showed that the pathological TDP-43 C-terminal fragments of 24 and 26 kDa in ALS and FTLD-TDP type A contain the epitope of anti-TDP-43 mAb, residues 203–209, by comparing the immunoblotting results with those using pS409/410 (Fig. 3). This result suggests that the cleavage sites of pathological TDP-43 C-terminal fragments in ALS and FTLD-TDP are located at the N-terminal side of Thr203. Although the mechanisms of generation of the C-terminal fragments are still controversial, the presence of multiple cleavage sites suggests that cleavage may occur after the aggregation or assembly of TDP-43.

Structural or conformational changes in the proteins are thought to be the most important in protein aggregation in these neurodegenerative diseases. To analyze the conformational change in the epitope of TDP-43 from normal to the abnormal states further, we treated the Sarkosyl-insoluble TDP-43 with trypsin or chymotrypsin, and immunoblotted with these antibodies. The protease-resistant TDP-43 bands and smears were detected in ALS and all subtypes of FTLD-TDP with these anti-TDP-43 antibodies (Fig. 4), while no such bands were seen in AD cases. These demonstrate that the epitope is protease-resistant in the abnormal TDP-43 but not in normal TDP-43. Using an antibody pS409/410 that recognizes the C-terminal phosphorylation sites, some protease-resistant TDP-43 bands are detected, and the band patterns are slightly different between ALS and FTLD-TDP type C [29]. On immunoblots with anti-TDP-43 pAb and mAb, such difference was not observed. This is probably due to that the epitope of the mAb and pAb is located in the amino-terminus of the protease-resistant core of the TDP-43, whereas epitope of the pS409/410 located in the C-terminus. Similar protease-resistant bands have been reported in abnormal prion in prion diseases, tau in Alzheimer's disease and alpha-synuclein in Parkinson's disease and dementia with Lewy bodies. Biochemical studies in these proteinopathies suggested that the protease-resistant bands represent the core domains of the filamentous aggregates of these proteins with cross-β structures [30–32]. By analogy with these proteins we propose that these protease-resistant C-terminal fragments represent the core of the filamentous aggregates of TDP-43. Since the epitope of the mAb and pAb are determined to locate at residues 203–209, this may be important in the formation of a core region of pathological TDP-43 aggregates which is common in all TDP-43 proteinopathies. Finally, the protease treatment used in this study may be useful for detection of the abnormal TDP-43 in brains of patients, animal models, culture cells and in vitro models with these anti-TDP-43 antibodies more specifically, as used for detection of abnormal prion proteins.

Acknowledgments

Authors thank Dr Tetsuaki Arai (Tsukuba University) for helpful advice and discussions. This work was supported by a Grant-in-Aid for Scientific Research (A) (to M.H., 11000624) from Ministry of Education, Culture, Sports, Science and Technology of Japan, and grants from Ministry of Health, Labor and Welfare of Japan (to M.H.).